01 Sep 1985

Design of automotive structural components using high strength sheet steels - results and evaluation of stub column tests for unstiffened curved elements

Wei-Wen Yu
Missouri University of Science and Technology, wwy4@mst.edu

M. Brad Parks

20 Parks, B.; Yu, W.
4 W.
15 DESIGN OF AUTOMOTIVE
02 STRUCTURAL
COMPONENTS USING
HIGH STRENGTH SHEET
STEELS -- RESULTS AND

Civil Engineering Study 85-1
Structural Series

Seventh Progress Report

DESIGN OF AUTOMOTIVE STRUCTURAL COMPONENTS USING HIGH STRENGTH SHEET STEELS

RESULTS AND EVALUATION OF STUB COLUMN TESTS FOR UNSTIFFENED CURVED ELEMENTS

by

Brad Parks
Research Assistant

Wei-Wen Yu
Project Director

A Research Project Sponsored by American Iron and Steel Institute

September 1985

Department of Civil Engineering

University of Missouri-Rolla

Rolla, Missouri

TABLE OF CONTENTS

TABLE OF CONTENTS (Cont.)

LIST OF TABLES

LIST OF TABLES (Cont.)

LIST OF TABLES (Cont.)

LIST OF FIGURES

LIST OF FIGURES (Cont.)

I. INTRODUCTION

A. GENERAL

In the past few years, a dramatic increase in the use of high strength sheet steels in automobiles has been brought about by the demand for improved fuel economy and safety of motor vehicles. Many of the automotive structural components, which are made of high strength sheet steels, consists either partially or totally of curved elements. Therefore, it was decided to include an investigation into the structural behavior of curved elements as a part of a research project entitled, "Structural Design of Automotive Structural Components Using High Strength Sheet Steels." The research project began in early 1982 at the University of Missouri-Rolla (UMR) under the sponsorship of the American Iron and Steel Institute (AISI). However, work did not begin on the curved element investigation until the spring of 1983. In August, 1983, the Fourth Progress Report of the research project entitled, "Preliminary Study of Members Consisting of Flat and Curved Elements[1]", was published. Included in this report was a review of all available literature on the behavior of curved elements as well as a tentative plan for an experimental investigation.

The Sixth Progress Report of the research project entitled, "Status Report on the Study of Members Consisting of Flat and Curved Elements[2]", was published in October, 1984. The Sixth Report contained an updated review of the literature along with a more definitive plan

for the experimental study. Particular emphasis was placed on the stub column testing, which had just begun at the time of printing.

Since the publication of the Sixth Progress Report, all of the proposed stub column tests (36) have been performed. However, there have been a few changes in the originally proposed experimental program. After close examination of the first few stub column tests, it was observed that, in some cases, the web actually buckled before the curved flanges. In order to prevent premature web buckling, vertical bracing was added to the web of approximately half of the stub column specimens. Therefore, no web buckling could occur in these sections. Since an investigation of the case in which the web buckled early also seemed desirable, the web was left unbraced on the remainder of the specimens. Thus, two types of failure patterns were studied for the stub column tests. First, the originally planned case in which the curved flange failed initially was investigated. Also studied was the interaction between the web and the curved flanges when the web buckled before the flange.

B. SCOPE OF INVESTIGATION

The primary purpose of this report is to discuss the research work that has been done on the study of curved elements since the issuance of the Sixth Progress Report.

Section II of the report summarizes the current status of the curved element research. Section III.A presents Redshaw's Equation (with some modification) and also an empirical equation determined by regression analysis of the stub column data. These equations are used to predict the local buckling strength of curved elements subjected to

uniform compression. Also discussed is an approximate procedure (Air Force Method) for predicting the total buckling load for sections consisting of flat and curved elements. Finally, a very brief discussion of the finite strip method, which might be useful for the prediction of curved element buckling, is presented.

Section III.B.1 describes the experimental program for the stub column specimens. In Section III.B.2, an evaluation of the stub column test results is given. An outline is proposed in Section IV for the design of cross-sections consisting of flat and unstiffened curved elements. Finally, a general summary of the curved element research is presented in Section V.

II. SUMMARY OF CURVED ELEMENT RESEARCH SINCE LAST REPORT

Since the issuance of the Sixth Progress Report, additional research work has been carried out in the following areas:

1) Completed the proposed stub column tests (36) of the last report.
2) Evaluation of the stub column data and subsequent formulation of an empirical equation for the prediction of the local, elastic buckling of unstiffened curved elements. The tangent modulus concept was used for the prediction of inelastic buckling.
3) Beam tests for the unstiffened curved elements (CB specimens) have begun.
4) Also being tested are stub columns which contain stiffened curved elements.
5) Began an initial study of the finite strip method for possible use in the analytical investigation of the buckling of curved elements.

At the time of writing, both the CB beam tests and the stub column tests for the stiffened curved elements are in progress. Because of the lengthy period of time required for milling the stub columns, the beam tests are performed between the stub column tests.

III. STRUCTURAL BEHAVIOR OF MEMBERS CONSISTING OF CURVED ELEMENTS

A. ANALYTICAL INVESTIGATION

1. Redshaw's Equation. The following information was originally presented in the Sixth Progress Report[2] and is recopied here, with a few revisions, to provide a complete report.

There have been several attempts to develop equations to predict the buckling stress of curved panels. Perhaps the most noteworthy of these equations was derived by Redshaw[4]. He developed the following expression on the basis of the classical energy approach:

$$f_{cr} = \frac{E}{6(1-\mu^2)}\left[\sqrt{12(1-\mu^2)\,\frac{t^2}{R^2} + \frac{\pi^4 t^4}{b^4}} + \frac{\pi^2 t^2}{b^2}\right] \qquad (3.1)$$

in which

f_{cr} = elastic buckling stress of a curved panel simply supported on all sides, ksi

E = modulus of elasticity, ksi

μ = elastic Poisson's ratio

t = curved element thickness, in.

R = curved element radius, in.

b = curved element arc length, in.

Sechler and Dunn[3] later showed that Eq. (3.1) could be expressed in terms of the flat plate and cylindrical buckling stresses as shown below:

$$(f_{cr}/E)_p = \sqrt{(f_{cr}/E)_c^2 + 1/4\ (f_{cr}/E)_f^2} + 1/2\ (f_{cr}/E)_f \qquad (3.2)$$

in which

$(f_{cr}/E)_p$ = buckling stress ratio of a simply supported curved element subject to uniform compression

$(f_{cr}/E)_c$ = buckling stress ratio of a full cylinder with the same R/t ratio as the curved element

$(f_{cr}/E)_f$ = buckling stress ratio of a simply supported flat plate with the same t/b ratio as the curved element

Because the theoretical buckling stress for cylinders,

$$f_{cr} = 0.6Et/R, \qquad (3.3)$$

consistently predicts f_{cr} values as much as twice the experimental values, it seems appropriate to replace the theoretical value of $(f_{cr}/E)_c$ with the following empirical relationship:

$$(f_{cr}/E)_c = 0.3t/R. \qquad (3.4)$$

As mentioned above, Eq. (3.1) was derived for a curved element, simply supported on all sides. For curved elements with one edge free, such as for the curved flanges of the stub columns described in Section III.B, Eq. (3.1) is reduced by the same ratio as for flat plates with similar boundary conditions. In other words, the buckling coefficient, k, for simply supported flat plates is 4.0 and for plates with one edge

free, k = 0.5. Therefore, Eq. (3.1) is multiplied by the factor 0.5/4.0 = 0.125 for curved elements with one edge free. Note that the value of k = 0.425, as originally proposed in the Sixth Progress Report[1], has been changed to 0.5. The reason for this change is that k = 0.5 seems to provide better agreement with the test data.

The above modifications have been incorporated into Eq. (3.1) to produce the following equation that will heretofore be referred to as the "modified Redshaw's Equation." The modified form of Redshaw's Equation, shown below, was used to predict the buckling stress of the curved flanges of the stub column specimens before testing. A representative cross-section for these specimens is shown in Fig. 3.4. Note that a value of 0.3 has been substituted for Poisson's ratio.

$$(f_{cr}/E_t)_{pm} = 0.0625\left[\sqrt{0.36(t/R)^2 + 13.07(t/b)^4} + 3.615(t/b)^2\right] \qquad (3.5)$$

2. Development of an Empirical Equation. After testing, a nonlinear, least squares regression analysis was made of the stub column data in which the curved elements failed elastically. Many combinations of the R, b, and t parameters were attempted. The equation that was found to best fit the data was also the simplest form of equation that was tried. This equation, which will be referred to as the "regression" equation, is shown below.

$$(f_{cr}/E_t)_{pm} = 0.02926(t/R) + 0.02090(t/b) \qquad (3.5a)$$

E_t in Eqs. (3.5) and (3.5a) represents the tangent modulus as later defined in Eq. (3.9), page 17. If $f_{cr} < F_{pr}$, use $E_t = E$.

Eq. (3.5a) was derived for the initial elastic buckling of the unstiffened curved elements of specimens having R/t ratios ranging from approximately 25 to 110 and b/t ratios ranging from approximately 25 to 90. The modulus of elasticity was assumed to be 29,500 ksi in both equations.

3. Air Force Method. Since curved elements are often used in combination with flat elements, as shown in Fig. 3.1, a systematic approach for the prediction of the critical buckling load of such sections is highly desirable. As discussed in the Fourth Progress Report[1], the most reasonable approach seems to be the Air Force Method. This method was originally published by Sechler and Dunn[3]. The following example describes the Air Force Method:

If, in the cross section shown in Figure 3.1(b), $f_{cr3}<f_{cr1}$ and $f_{cr3}<f_{cr2}$, then the critical stress will be

$$f_{cr} = \frac{f_{cr3}(2A_1 + 2A_2 + A_3)}{2A_1 + 2A_2 + A_3} = f_{cr3} \tag{3.6}$$

If $f_{cr1}<f_{cr3}$ and $f_{cr2}>f_{cr3}$, the critical stress will be

$$f_{cr} = \frac{f_{cr1}(2A_1) + f_{cr3}(2A_2 + A_3)}{2A_1 + 2A_2 + A_3} \tag{3.7}$$

If $f_{cr1}<f_{cr3}$ and $f_{cr2}<f_{cr3}$, the critical stress will be

$$f_{cr} = \frac{f_{cr1}(2A_1) + f_{cr2}(2A_2) + f_{cr3}(A_3)}{2A_1 + 2A_2 + A_3} \tag{3.8}$$

As shown by this example, the curved elements are assumed to have no post-buckling strength; thus, when the first curved element reaches its buckling stress, the total capacity of the section is reached. Should a flat element buckle before the curved element, the flat element is assumed to carry its buckled load (without additional gain in post-buckling strength) until the critical stress is reached in a curved element. Of course, the maximum value of any of the above stresses is limited to the yield strength of the material.

4. Finite Strip Method. Since the analytical prediction of the buckling behavior of curved elements is, at best, approximate, it seems that some sort of numerical technique will be necessary for the accurate prediction of curved element buckling. In the Sixth Progress Report[2], a brief summary of available commercial finite element programs was presented. Since then, an additional investigation into the capabilites of the finite strip method has begun. The finite strip method has proven to be very effecient and successful for the prediction of flat plate initial buckling and post-buckling[9-11]. With some modification, it may be possible to use this same approach for the problem of curved element buckling. Obviously, considerable study remains to be done in this area.

B. EXPERIMENTAL INVESTIGATION OF UNSTIFFENED CURVED ELEMENTS:

STUB COLUMN TESTS

1. Description of Stub Column Tests.

a. Specimens. All of the curved element specimens were formed by Wania Ornamental Wire and Iron Co. in St. Louis, Missouri. A press brake operation, which employed a series of circular "pipe" dies, was

used to form the curved elements. As presented in the Sixth Progress Report[2], Tables 3.2 and 3.3 provide a summary of all curved element specimens. The mechanical properties for the materials used in these specimens are listed in Table 3.1. Figures 3.2 thru 3.5 show the typical cross-sections for all specimens.

Stub column tests for the CS profile, shown in Fig. 3.4, are the primary consideration in this report. Table 3.2 lists the three basic radii of the CS curved flanges (R=1", 1.25", or 4"). The three different radii may be compared in Fig. 3.10. As shown in Table 3.3, a minumum of two tests have been performed for each radius and material.

The specimen designation is best explained by the following example. For the 80XFCS3-1B specimen, the first four characters represent the AISI material designation[8]. The next three characters, "CS3" in this case, identify both the type of section (CS = stub column, Fig. 3.4) and the curvature of the flange (for instance, "3" signifies R=1"). The following digit represents the specimen number for each type of section. The final letter in the designation indicates whether the stub column specimen is braced, "B", or unbraced, "U". Note that, for the 50XF materials, the nominal thickness (in thousansandths of an inch) is also included in the specimen designation (in parenthesis) to distinguish between the two materials.

The radii of the CS1 specimens were measured directly by comparing the inner surface of the curved flanges with a "radius gage" similar to that shown in Fig. 3.6. For the CS2 and CS3 specimens, the radii could be more accurately determined by measuring the arc and chord lengths of the flanges and then computing the radii based on these values. Using

this procedure, the radius and arc length of the ends of the curved flanges were measured. These values were then averaged for each flange. The average values, along with the thickness, web depth, and area are presented in Table 3.4. The four different flanges of each stub column are identified as shown in Fig. 3.9. The stub columns were approximately 12 in. long.

As illustrated in Fig. 3.4, the CS specimens were fabricated from two individual "channel" type sections. Self-tapping screws (#14 x 3/4) were used to connect the channels. Three vertical columns of fasteners, spaced 2 in. apart vertically, were used for all stub column specimens. Originally, only two columns of fasteners were believed to be necessary for the CS1 specimens. However, because of lower than expected web buckling stresses, three columns were used in order to increase the strength of the web. For all CS specimens, the outer vertical columns were placed as close as practicable to the edge of the web. Figure 3.7 shows the fastener arrangements for the CS specimens.

Once fabricated, the ends of the stub columns were milled flat and parallel, with their longitudinal axis perpendicular to the milled ends. Flatness of the ends was checked by placing the stub columns on a flat, level surface and observing any rock or light that might be visible between the specimen and the flat surface. If the ends were not found to be flat, the milling procedure was repeated until the ends were made as flat as possible.

After performing a few stub column tests, it was observed that the web failed at lower than expected stresses and, in some cases actually failed before the adjoining curved flanges. Since the early failure of

the web definitely has an effect on the overall failure load of the specimens, vertical bracing (3/4 X 3/4 X 1/8") was attached to the web in order to prohibit web buckling. The bracing was added to approximately one-half of the stub column specimens. Figures 3.11 and 3.12 show the attachment of the bracing. As shown, each brace was connected to the web by three 1/4" dia. bolts. The upper and lower bolt holes were elongated so that the bracing would pick up no load from the web. Also, a thin layer of aluminum foil, coated with WD-40, was placed between the web and the brace. Inspection of the strain output from gages 13 and 14 (Fig. 3.9), which were located at the center of the web, verified that the bracing did indeed not carry any load.

By adding bracing to some of the specimens, two different types of failure modes occurred. For the unbraced specimens, the web was allowed to buckle before the curved flange and thus, the interaction of the web and flange could be studied. Meanwhile, the curved flanges of the braced specimens always failed before the web.

b. Strain Measurements. Fourteen foil strain gages were used to measure strains at midheight of the stub column specimens. The gage locations are shown in Fig. 3.9. The critical buckling stress for the curved elements was found by using the modified strain reversal method (described in Ref. 6) for the strain output of the paired gages located on each side of the flange tips. Also, the location of the first failed flange was identified as a result of this procedure.

Additional strain gages were placed at or close to the webs of the specimens so that the average strains associated with buckling could be measured. All of the strain gages were used in the procedure for aligning the specimens as described in Section 3.B.1.e.

c. Waving and Deformation Measurements. Out-of-plane waving of the curved flange tips was recorded at thirteen points along the length of each flange. At each point, the wave deformation was measured by a horizontally mounted linear variable differential transformer (LVDT) that is attached to a moveable vertical stand. The height of the LVDT was adjusted by sliding along the vertical stand. In order to measure waving of all four flanges, the base of the stand was placed in a slotted block adjacent to each flange. The widths of the slots were such that the vertical stand base fit snuggly in the slot and thus no torsional rotation of the stand could occur. The purpose of the slotted blocks was to maintain a fixed reference point from which waving could be measured at several load levels.

Before testing, the LVDT (with vertical stand base in the slotted block) was oriented such that its axis was perpendicular to the desired flange; the slotted block was then clamped to the base of the testing machine. After clamping, the vertical stand was moved to the next flange and the same procedure repeated there. The completed setup for the measurement of waving is shown in Fig. 3.13. Using the above procedure, both the wave depth and shape could be determined for any load level.

Wave readings were recorded at four typical load levels for each test: (1) at the beginning of each test with no load on the specimen, (2) at approximately half the predicted failure load, (3) shortly after initial buckling of the first curved flange, and (4) at overall failure of the specimen. In many cases, (3) and (4) occurred simultaneously such that only one set of readings was possible at failure.

Also, lateral deflection of the web (for unbraced specimens) and cross head movement were recorded at each load level. These measurements were used to monitor the overall performance of the specimen and to check the appropriate instrumentation.

d. Equipment. All but four of the stub column specimens were tested in the 120,000 pound Tinius Olsen testing machine located in the Engineering Research Laboratory at UMR. Figure 3.14 shows the testing machine along with the remaining equipment used in the stub column tests. The four remaining specimens, because of their relatively high expected failure load, were tested in a 200,000 pound Tinius Olsen testing machine located in the Materials Laboratory of the Civil Engineering Building at UMR. The accompanying equipment was exactly the same as shown in Figure 3.14.

An Electronics/Ltd., 40 channel data acquisition system (Fig. 3.15) was used to measure the strain gage output. An additional acquisition system (Fig. 3.16) measured the load output from the Tinius Olsen machine and the waving from the LVDT. The IBM Personal Computer (Fig. 3.17) was used to coordinate the electronic equipment and store the load, strain, and wave output at each measured load level.

e. Test Procedure. Before fabrication, each of the paired channel specimens were measured individually as described in Section 3.B.1.a. Once measured, the channels were connected, as previously described, and their ends were milled flat. After attaching the strain gages, the stub column was placed in the Tinius Olsen machine. Flat, hardened steel base plates provided the bearing surface for the ends of the specimens. The strains were made uniform over the stub column cross-

section by the following procedure. First, a small preload was applied and the resulting strains recorded for all strain gages. If necessary, thin layers of aluminum foil were added to the regions of low strain. This procedure was repeated until the strain distribution was essentially uniform over the cross-section.

Next, the slotted blocks, which were used in the measurement of waving, were positioned and then clamped to the lower table of the Tinius Olsen machine. The test setup is shown in Fig. 3.13. At this point the test was ready to begin.

As mentioned earlier, the load was applied by either a 120,000 or 200,000 pound Tinius Olsen testing machine. The load increments were such that a minimum of ten load levels were measured before failure of the specimen. Between load levels, the load was increased very slowly so that any strain rate effect on the mechanical properties was negligible. Once the desired load level was reached, the load was held constant for a period of time to allow the specimen to stabilize.

At each load level, load and the corresponding strains were recorded and stored by the computer. Wave readings were measured by the LVDT as described in Section 3.B.1.c. at the beginning of the test, at approximately one-half of the failure load, and at or close to failure of the specimen. Between wave readings, a stationary dial gage, placed near midheight of one of the curved flanges, was used to monitor the movement of the flange. Also measured at each load level was the cross head movement and lateral deflection of the web (for unbraced specimens). The ultimate load was taken directly from the Tinius Olsen machine as the maximum load that the specimen could withstand.

2. Discussion of Stub Column Test Results. As mentioned earlier, two types of failure patterns occurred for the stub column tests. In the first case, premature failure of the web was prohibited, if necessary, by attachment of vertical bracing to the webs (Fig. 3.11); thus, for all such tests the curved flanges were the initial and final cause of failure. The results of these tests are discussed below in Section 3.B.2.a. The other type of failure occurred when the unbraced web of some of the specimens actually buckled before the adjoining curved flanges. Section 3.B.2.b. analyzes the results of these tests. It should be noted that the webs of all unbraced specimens did not buckle before the adjoining curved elements.

a. Initial Curved Element Failure. The results of the stub column tests in which the curved element buckled before the web are given in Table 3.6. Column (2) of this table lists the initial buckling loads associated with the first curved flange buckle. The magnitude of the buckling load was determined by the modified strain reversal method[6].

The ultimate load that the specimen could withstand was taken directly from the Tinius Olsen machine and is recorded in column (1). Column (6), which is the ultimate divided by the initial buckling load, gives some idea of the magnitude of the post-buckling strength of the curved elements. There seems to be a gradual increase in post-buckling strength as the curvature of the flange decreases. For example, the CS3 (R=1") specimens show no appreciable post-buckling strength whereas the CS1 specimens (R=4") show an approximate 20% increase above the initial buckling load. This sort of behavior is not unexpected, since highly

curved structural elements (such as cylinders) are noted for their lack of post-buckling strength while flat, unstiffened elements may exhibit considerable strength after buckling.

The yield strength, F_y, and the proportional limit, F_{pr}, along with R/t and b/t are given in Table 3.5 for each of the specimens that failed by initial curved element buckling. The "First Flange" column lists the position on the cross-section (Fig. 3.9) of the first buckled flange. In some cases, there was no measureable flange buckling before collapse of the section. In these cases, "NONE" is recorded in this column.

i. Comparison of Prediction Equations to Initial Buckling Loads. Two different equations, Eq. (3.5) (modified Redshaw's Eq.) and Eq. (3.5a) (regression Eq.), are compared to the initial buckling of the curved elements. For each equation, three different approaches were employed. In the first approach, perfect elastic-plastic action of each material is assumed. In other words, elastic buckling is assumed up until $f_{cr} = F_y$ (for $f_{cr} > F_y$, use $f_{cr} = F_y$).

In the second and third approaches, the tangent modulus, E_t, is substituted for the elastic modulus, E, when $f_{cr} > F_{pr}$. The tangent modulus equation is given below.

$$E_t = E \frac{(f_{cr}/F_y)(1-(f_{cr}/F_y))}{(F_{pr}/F_y)(1-(F_{pr}/F_y))} \tag{3.9}$$

The second approach uses the actual values of F_{pr} and F_y for each material (Table 3.5), as determined by longitudinal compression tests, to compute E_t. Finally, the third approach assumes $F_{pr} = 0.7F_y$. In each case, the predicted initial buckling load is computed as the

predicted buckling stress from the appropriate equation times the total cross-sectional area of the specimen. The predicted initial buckling loads for each equation and approach are presented in Tables 3.6 thru 3.11. The following is a summary of the information provided in these tables.

Table	Description
3.6	Modified Redshaw's Eq. (3.5) assuming elastic-plastic action
3.7	Modified Redshaw's Eq. (3.5) $E = E_t$, F_{pr} and F_y of each mat'l
3.8	Modified Redshaw's Eq. (3.5) $E = E_t$, $F_{pr} = 0.7F_y$
3.9	Regression Eq. (3.5a) assuming elastic-plastic action
3.10	Regression Eq. (3.5a) $E = E_t$, F_{pr} and F_y of each mat'l
3.11	Regression Eq. (3.5a) $E = E_t$, $F_{pr} = 0.7F_y$

For the curved elements that failed by elastic buckling, $E_t = E$, and thus only Tables 3.6 and 3.9 need be compared. As shown in Table 3.6 (column(4)), the modified Redshaw's Eq. (3.5) provides good estimates for the initial, elastic buckling of the CS3 and CS2 specimens. However, for the flatter CS1 specimens the predicted values are considerably lower than the test values. The mean value, shown in Table 3.6 for column (4), reflects the influence of the low predicted loads for the CS1 specimens.

In order to improve the prediction for the flatter curvatures, a nonlinear least squares regression analysis, as described in Section 3.A.1, was performed on the stub column data in which elastic buckling occurred. The resulting regression Eq. (3.5a) is compared to the test results in column (4) of Table 3.9. As shown, Eq. (3.5a) provided

equally good agreement with the data for the CS3 and CS2 specimens. However, considerable improvement was obtained in the predicted values for the flatter CS1 specimens. This improvement is particularly evident in the mean value of the tested-to-predicted values in Table 3.9.

As shown in Tables 3.6 and 3.9, when perfect elastic-plastic action is assumed, a considerable overestimation of the buckling load may result for the specimens that are assumed to fail by yielding ($f_{cr} > F_y$). In fact, these specimens typically failed at 80-85% of the yield stress for a given material. A more accurate, but time consuming approach is to use some sort of reduced modulus of elasticity for the sections that fail inelastically ($f_{cr} > F_{pr}$). In Tables 3.7, 3.8, 3.10, and 3.11, the elastic modulus has been replaced by the tangent modulus (Eq. 3.9) in the respective equations when $f_{cr} > F_{pr}$. In Tables 3.7 and 3.10, the actual values of F_{pr} and F_y for each material were used in the calculation of E_t. A more general value of $F_{pr} = 0.7F_y$ was assumed in Tables 3.8 and 3.11. As expected, the use of the actual values of F_{pr} and F_y provide better agreement than $F_{pr} = 0.7F_y$; however, either method yields considerable improvement in the predicted inelastic buckling values.

In order to better compare the various methods for predicting the initial buckling load of the unstiffened curved elements, Table 3.12 lists the tested-to-predicted ratios as computed by the modified Redshaw's Eq. (3.5) and the regression Eq. (3.5a) for each approach. As shown, the regression Eq. (3.5a), with $E = E_t$ and using F_{pr} and F_y of each material (Table 3.10), provides the best overall agreement with the test data. However, Eq. (3.5a) with $E = E_t$ and $F_{pr} = 0.7F_y$ (Table 3.11) is a more general approach and, because it also provides reasonably

accurate predictions of the initial buckling loads, this approach is recommended. The initial buckling loads are compared to the predicted buckling loads, which were computed using this method, in Figures 3.24 thru 3.26.

ii. Comparison of Prediction Equations to Ultimate Loads. Because the current trend in design specifications is to base all calculations on the ultimate strength of a structure, the ultimate load recorded for each stub column specimen has been compared to the predicted buckling load. The reason for the comparison is to determine if the predicted buckling loads, as computed by the modified Redshaw's Eq. (3.5) or the regression Eq. (3.5a), are adequate for the prediction of the ultimate load of the stub column specimens. The ultimate-to-predicted load ratios for each equation and approach are listed in column (5) of Tables 3.6 thru 3.11. Table 3.13 summarizes the ultimate-to-predicted load ratios for each method.

As expected, for those specimens with little, if any, post-buckling strength, there is no appreciable difference in the accuracy of the prediction from the initial buckling case. However, for the flatter CS-1 specimens, which exhibited considerable post-buckling strength, the modified Redshaw's Eq. (3.5) is extremely conservative. The regression Eq. (3.5a) is much less conservative for these specimens. As shown for Table 3.10, the regression Eq., with $E = E_t$ and using F_{pr} and F_y of each material, provides the best overall agreement with the ultimate loads. However, the use of $E = E_t$ and $F_{pr} = 0.7F_y$ in Eq. (3.5a) (Table 3.11) is recommended because it is a more general approach and because it also provides reasonably accurate predictions of the ultimate loads. Figures 3.27 thru 3.29 provide a comparison of the

ultimate loads with the predicted buckling loads, which were computed using this method.

iii. Typical Failure Modes. The CS3 and CS2 specimens typically exhibited very little, if any, waving of the free edge of the curved element prior to initial buckling. In all cases, the magnitude of the wave depth was less than the respective thickness of the materials. Figure 3.18 shows the buckled flange of a typical specimen. The wave pattern, as recorded by the LVDT, of representative tests for the CS3 and CS2 specimens are given in Figures 3.19 and 3.20, respectively.

The CS1 specimens also showed very little waving before initial buckling. However, after initial buckling and before the ultimate load, waving of the curved flange tips became much more pronounced. Figure 3.21 shows the buckled configuration of a CS1 specimen at its ultimate load. A typical wave pattern measured by the LVDT at close to the ultimate load is given in Figure 3.22.

As mentioned earlier, the cross head movement of the Tinius Olsen machine was recorded at each load level. Although not directly used in the calculations, the cross head movement was monitored in order to detect the onset of any nonlinear behavior in the specimen. As expected, buckling of the curved flanges occurred soon after the beginning of nonlinear cross head movement. A typical plot of load versus cross head movement is given in Fig. 3.23.

b. Initial Flat Element Failure. Table 3.15 presents the results of the stub column tests in which the flat web failed before the initial curved flange buckle. As previously described for Table 3.6, columns (1) and (2) lists the ultimate and initial curved element buckling

loads, respectively. Again, the magnitude of the initial curved element buckling load was determined by the modified strain reversal method.

Although not included in Table 3.15, a comparison of the ultimate-to-initial buckling loads reveals a similar trend in post-buckling strengths as for the previously described case in which the curved element buckled first. In other words, there was no appreciable post-buckling strength for the CS3 and CS2 specimens, whereas the CS1 specimens did have some additional strength after buckling.

The properties, F_y and F_{pr}, along with R/t and b/t are given in Table 3.14 for each of the specimens that failed by initial flat element buckling. The "First Flange" column is the same as described for Table 3.5.

i. Comparison of Prediction Equations to Initial Buckling. According to the Air Force Method[3], which was described in detail in Section 3.A.3, the total load that a cross-section, consisting of flat and curved elements, can withstand is obtained when the first curved element reaches its respective buckling stress. Thus, no post-buckling strength whatsoever is assumed for the curved elements. If one or more of the flat elements buckle before the curved element, the buckled flat elements are assumed to maintain their load until the curved element buckling stress is reached. This same general procedure has been adopted for the prediction of the total load of the stub column specimens in which the web buckled before the curved flanges.

In order to compute the total load resisted by the web, the effective width approach, as given in Section 2.3.1.1 of the 1980 AISI Specification[7], was employed. The effective width equation recommended by AISI is shown below:

No reduction in width is required if $(w/t) < (w/t)_{lim} = 221/\sqrt{f}$

If $(w/t) > (w/t)_{lim}$

$$b_e = \frac{326t}{\sqrt{f}}\left[1 - \frac{71.3}{(w/t)\sqrt{f}}\right] \qquad (3.10)$$

in which:

w = full width of compression element, in.

t = thickness, in.

b_e = effective width, in. (Fig. 3.8)

f = actual stress at the edge of compression element, ksi.

The edge stress, f, used in the effective width equation was the predicted curved element buckling stress, as determined from either Eq. (3.5) or (3.5a). Twice the material thickness was used for t since the web consists of two connected flat elements. Thus, the predicted web load, P_w, (column (3) of each table) was computed as the edge stress, f, times the effective web area, $2b_e t$.

The predicted curved element buckling stress was calculated by three different approaches, just as for the initial curved element failure, using first the modified Redshaw's Eq. (3.5) and then the regression Eq. (3.5a). In each case, P_{curve} was calculated as the curved element buckling stress from the respective prediction equation, times the total curved element area. Finally, the total predicted buckling load, P_{total}, is simply P_w plus P_{curve}.

The predicted values of P_{total}, along with the initial buckling-to-predicted load ratios (column (6)) for each equation and approach are given in the tables listed below. The mean and standard deviation of the initial buckling-to-predicted load ratios are provided for each table.

Table	Description
3.15	Modified Redshaw's Eq. (3.5) assuming elastic-plastic action
3.16	Modified Redshaw's Eq. (3.5) $E = E_t$, F_{pr} and F_y of each mat'l
3.17	Modified Redshaw's Eq. (3.5) $E = E_t$, $F_{pr} = 0.7F_y$
3.18	Regression Eq. (3.5a) assuming elastic-plastic action
3.19	Regression Eq. (3.5a) $E = E_t$, F_{pr} and F_y of each mat'l
3.20	Regression Eq. (3.5a) $E = E_t$, $F_{pr} = 0.7F_y$

As in the case of initial curved element buckling, the insertion of the tangent modulus for those specimens with $f_{cr} > F_{pr}$ produced some improvement in the predicted buckling values. Both the modified Redshaw's Eq. (3.5) and the regression Eq. (3.5a) seem to provide equally good predictions for the inelastic buckling and also for the elastic buckling of the CS3 and CS2 specimens. However, for the elastic buckling of the CS1 specimens, the regression Eq. (3.5a) again gives closer predictions than the modified Redshaw's Eq. (3.5) except for the 30SKCS1-1U specimen. For some unknown reason, this specimen failed at a much lower than expected load. Since the results of this test are suspect, it was not included in the computation of the mean and the standard deviation.

Table 3.21 lists the initial buckling-to-predicted load ratios, as computed by each approach using the modified Redshaw's Eq. (3.5) and the regression Eq. (3.5a), for those specimens that experienced initial web buckling. Note that although the mean values for the modified Redshaw's Eq. is closer to 1.0 than for the regression Eq., the standard deviations of Eq. (3.5a) are substantially lower. Therefore, the regression Eq. (3.5a) with $E = E_t$ and $F_{pr} = 0.7F_y$ (Table 3.20) is

recommended. The initial buckling loads are compared to the total predicted loads, which were computed using this method, in Figures 3.30 thru 3.32.

ii. Comparison of Prediction Equations to Ultimate Loads. Again, because the current trend in design specifications is to base all calculations on the ultimate strength of a structure, the ultimate load that each stub column specimen could withstand has been compared to the total predicted load of each specimen. The primary purpose of the comparison is to determine if the total predicted loads, P_{total} are adequate for the prediction of the ultimate load. The ultimate-to-predicted load ratios for each equation and approach are listed in column (7) of Tables 3.15 thru 3.20. Table 3.22 summarizes these values for each table.

As shown in Table 3.22, the mean values of the predicted total load, based on the modified Redshaw's Eq. (3.5) (Tables 3.15 thru 3.17), are closer to 1.0 than the respective values for the regression Eq. (3.5a) (Tables 3.18 thru 3.20), However, because of the relatively high standard deviations associated with Eq. (3.5), this equation is not recommended. The regression Eq. (3.5a) with $E = E_t$ and $F_{pr} = 0.7F_y$ (Table 3.20) provides the best overall agreement with the ultimate loads and thus, this approach is recommended. Figures 3.33 thru 3.35 provide a comparison of the ultimate failure loads to the predicted total loads, which were calculated using this method.

iii. Typical Failure Modes. As far as the curved elements are concerned, their failure modes were practically identical to the previously described case where the curved elements failed first. After

initial buckling of the web, the overall cross-section remained stable with very little waving until the critical stress of the curved elements was reached. At that load (or very near this load), the ultimate load was obtained for the CS3 and CS2 specimens. As evidenced by columns (1) and (2) of Table 3.15, there was a slight amount of post-buckling strength, which was accompanied by significant waving, for the CS1 specimens.

IV. PROPOSED DESIGN RECOMMENDATIONS

The following is a recommended outline for the design of cross-sections composed of flat and unstiffened curved elements which are subjected to uniform axial compression.

1) Using Eq. (3.5a), with $E = E_t$ and $F_{pr} = 0.7F_y$, compute the minimum predicted buckling stress for all of the unstiffened curved elements, $(f_{cr})_{pm}$.
2) Compute $(w/t)_{lim}$, using the appropriate AISI equation for the flat elements with $(f_{cr})_{pm}$ as the edge stress.
3) If no reduction in w/t is required (i.e., $w/t < (w/t)_{lim}$), then assume that the section fails by initial buckling of the unstiffened curved element. Therefore, the total capacity of the column is $(f_{cr})_{pm}$ times the total cross-sectional area.
4) If $w/t > (w/t)_{lim}$, compute the effective width of the flat elements using the appropriate AISI equation. The total load resisted by the flat elements, P_w, equals the effective width times the respective thickness times the assumed edge stress, $(f_{cr})_{pm}$. The load resisted by the curved elements, P_{curve}, equals $(f_{cr})_{pm}$ times the respective curved element areas. Finally, the total load that the section can withstand, P_{total}, is simply P_w plus P_{curve}.

It should be noted that the regression Eq. (3.5a) is an empirical expression developed for the following ranges of R/t and b/t:

$$25 < R/t < 110$$

$$25 < b/t < 90$$

Therefore, use of Eq. (3.5a) should be restricted to these limits.

V. CONCLUSIONS

Because many automotive structural components contain curved elements in their cross section, it was decided to include an investigation of the structural behavior of these elements as a part of a research project at the University of Missouri-Rolla. The research project began in early 1982 under the sponsorship of the American Iron and Steel Institue. In the spring of 1983 work began on the curved element research. The Fourth Progress Report[1], published in August, 1983, presented a review of the literature on the structural behavior of curved elements. In October, 1984, the Sixth Progress Report[2] was published. This report presented a detailed look at the proposed experimental program for the study of curved elements with particular emphasis on the stub column testing.

The primary purpose of the present report was to update the status of the curved element research. Section II provided a brief summary of the curved element research work that has occurred since the issuance of the Sixth Progress Report. Section III.A described an approximate procedure that was to be used for the prediction of the curved element buckling. Also included was a very brief review of the finite strip method.

In Section III.B.1, the stub column testing procedure was discussed in detail. The results of the stub column tests were evaluated in Section III.B.2. From this evaluation it was shown that, when the curved elements buckled initially, both the modified Redshaw's

Eq. (3.5) and the empirically obtained regression Eq. (3.5a) provided good agreement with the test data for the elastic buckling of the CS3 and CS2 specimens. However, the regression Eq. (3.5a) produced much better agreement with the test results for the flatter CS1 specimens. For those specimens that failed by inelastic buckling, the use of the tangent modulus concept in Eq. (3.5) and Eq. (3.5a) provided good agreement with the test results. For the case in which the web buckled initially, the Air Force Method, using either Eq. (3.5) or Eq. (3.5a) for the curved elements, produced fair estimates of the total buckling load of the stub columns. After comparing Eq. (3.5) and (3.5a) for each approach, Eq. (3.5a) with $E = E_t$ and $F_{pr} = 0.7F_y$ was selected as the recommended equation for the prediction of unstiffened curved element buckling.

Finally, Section IV presented a general outline for the prediction of the total load that a section consisting of flat and unstiffened curved elements can withstand.

As mentioned earlier, stub columns, composed of stiffened curved elements, and the CB beam tests are currently being tested. Once completed, the A and D beam specimens and the B shear specimens will be tested.

ACKNOWLEDGMENTS

The research work reported herein was conducted in the Department of Civil Engineering at the University of Missouri-Rolla under the sponsorship of the American Iron and Steel Institute.

The financial assistance granted by the Institute and the technical guidance provided by members of the AISI Task Force on Structural Design and Research of the Transportation Department and the AISI staff are gratefully acknowledged. These members are: Messrs. S. J. Errera, D. M. Bench, A. E. Cornford, Jim Davidson, Charles Haddad, Emil Hanburg, Al Houchens, L.J. Howell, A. L. Johnson, R. G. Lang, B. S. Levy, Kuang-Huei Lin, Hickmat Mahmood, Don Malen, D. J. Meuleman, M. S. Rashid, Joe Rice, W. J. Riffe, Robin Stevenson, Brian Taylor, R. J. Traficanti, T. L. Treece, M. T. Vecchio and David Whittaker.

All materials used in the experimental study were donated by Bethlehem Steel Corporation, Inland Steel Company, and National Steel Corporation.

Appreciation is expressed to Messrs. K. Haas, J. Tucker, and R. Haselhorst, staff of the Department of Civil Engineering, for their support. The assistance provided by Mr. C. Santaputra in the performance of the stub column tests is greatly appreciated.

BIBLIOGRAPHY

1. Parks, M.B., and Yu, W.W., "Design of Automotive Structural Components Using High Strength Sheet Steels: Preliminary Study of Members Consisting of Flat and Curved Elements," Fourth Progress Report, Civil Engineering Study 83-5, University of Missouri-Rolla, August, 1983.

2. Parks, M.B., and Yu, W.W., "Design of Automotive Structural Components Using High Strength Sheet Steels: Status Report on the Study of Members Consisting of Flat and Curved Elements," Sixth Progress Report, Civil Engineering Study 84-2, University of Missouri-Rolla, October, 1984.

3. Sechler, E.E., and Dunn, L.G., Airplane Structural Analysis and Design, New York, NY: John Wiley & Sons, Inc., 1942.

4. Redshaw, S.C., "The Elastic Stability of a Curved Panel Under Axial Thrust", The Aeronautical Journal, Vol. 42, pp. 536-553, 1938.

5. Yu, W.W., Santaputra, C., and Parks, B., "Design of Automotive Structural Components Using High Strength Sheet Steels," First Progress Report, Civil Engineering Study 83-1, University of Missouri, January, 1983.

6. Johnson, A.L., "The Structural Performance of Austentic Stainless Steel Members," Department of Structural Engineering Report No. 327, Cornell University, November, 1966.

7. American Iron and Steel Institute, "Specification for the Design of Cold-Formed Steel Members," 1980 Edition.

8. American Iron and Steel Institute, "High Strength Sheet Steel Source Guide," SG-603D.

9. Cheung, Y.K., Finite Strip Method in Structural Analysis, Pergamon Press, 1976.

10. Sridharan, S. and Graves-Smith, T. R., "Post-Buckling Analysis with Finite Strips," Journal of the Engineering Mechanics Division, ASCE Proceedings, Vol. 107, No. EM5, October, 1981.

11. Benito, R., and Sridharan, S., "Interactive Buckling with Finite Strips," International Journal for Numerical Methods in Engineering, Vol. 21, 1985.

Table 3.1

Material Properties* and Thicknesses of Six

Sheet Steels to Be Used for Curved Element Tests

Material Designation	F_y (ksi)	F_u (ksi)	Elongation*** (%)	t (in.)
30SK	26.5	44.7	45.7	0.030
50XF(39)**	54.2	63.1	33.3	0.039
50XF(78)	57.2	66.5	27.3	0.078
80SK	82.2	88.8	12.7	0.061
80DK	58.2	87.6	25.7	0.048
80XF	88.3	98.7	22.8	0.082

* Material properties are based on the average longitudinal tension tests.

** Numbers in parenthesis indicate the nominal thicknesses in thousandths of an inch.

*** Elongation was measured over a 2 in. gage length.

Table 3.2

Dimensions of Test Specimens Consisting

of Curved Elements

Specimen No.	R (in.)	b (in.)	Length (in.)	Load Type
A1	15	4.01	60	Bending
A2	3.5	4.26	60	Bending
A3	2	6.29	60	Bending
B1	15	4.01	30	Shear
B2	3.5	4.26	30	Shear
B3	2	6.29	30	Shear
CS1	4	2.02	12	Compression
CS2	1.25	2.32	12	Compression
CS3	1	3.14	12	Compression
CB1	4	2.02	60	Bending
CB2	1.25	2.32	60	Bending
CB3	1	3.14	60	Bending
D1	2	3.14	60	Bending
D2	2	4.19	60	Bending

Table 3.3

Number of Tests for Each Material

Specimen No.	Material Designation						
	30SK	50XF(39)	50XF(78)	80SK	80DK	80XF	Total
A1	2	2	2	2	2	2	12
A2	2	2	2	2	2	2	12
A3	2	2	2	2	2	2	12
B1	2	2	2	2	2	2	12
B2	2	2	2	2	2	2	12
B3	2	2	2	2	2	2	12
CS1	2	2	2	2	2	2	12
CS2	2	2	2	2	2	2	12
CS3	2	2	2	2	2	2	12
CB1	2	2	2	2	2	2	12
CB2	2	2	2	1	2	2	11
CB3	2	2	2	2	2	2	12
D1	2	2	2	-	2	2	10
D2	2	2	2	-	2	2	10
TOTAL	28	28	28	23	28	28	163

DESIGNATION OF TEST SPECIMENS USED IN TABLES 3.4 THRU 3.6A

Specimen:

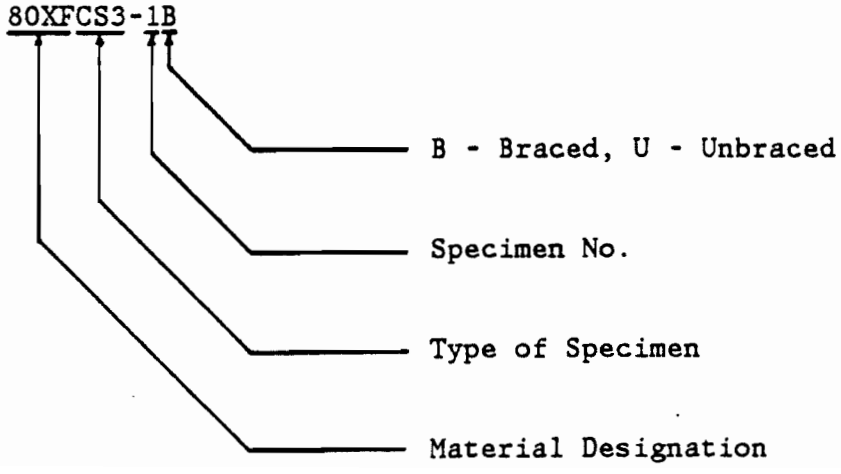

Table 3.4

Measured Dimensions of Stub Column Specimens

Specimen	Web Depth (in.)	Thickness (in.)	Area ($in.^2$)	Flange	Arc Length (in.)	Radius (in.)
80XFCS3-1B	4.15	0.087	1.83	ATOP	3.43	1.05
				ABOT	3.39	1.08
				BTOP	3.39	1.06
				BBOT	3.28	1.06
80XFCS3-2B	4.10	0.087	1.81	ATOP	3.23	1.11
				ABOT	3.24	1.04
				BTOP	3.22	1.10
				BBOT	3.37	1.05
50XF(78)CS3-3B	4.10	0.080	1.67	ATOP	3.36	1.01
				ABOT	3.34	1.03
				BTOP	3.29	1.03
				BBOT	3.23	1.025
50XF(78)CS3-1U	4.20	0.079	1.64	ATOP	3.16	1.03
				ABOT	3.21	1.03
				BTOP	3.23	1.04
				BBOT	3.24	1.03
80SKCS3-2B	4.05	0.062	1.29	ATOP	3.27	1.03
				ABOT	3.35	1.06
				BTOP	3.30	1.03
				BBOT	3.35	1.05
80SKCS3-3U	4.20	0.061	1.28	ATOP	3.18	1.08
				ABOT	3.34	1.04
				BTOP	3.35	1.07
				BBOT	3.34	1.04
80DKCS3-2B	4.05	0.046	0.964	ATOP	3.14	1.08
				ABOT	3.34	1.04
				BTOP	3.30	1.04
				BBOT	3.17	1.08
80DKCS3-3U	4.10	0.047	0.975	ATOP	3.25	1.12
				ABOT	3.20	1.09
				BTOP	3.20	1.09
				BBOT	3.33	1.09
50XF(39)CS3-3B	4.20	0.039	0.812	ATOP	3.12	1.04
				ABOT	3.17	1.03
				BTOP	3.10	1.02
				BBOT	3.26	1.04

Table 3.4 (Cont.)

Measured Dimensions of Stub Column Specimens

Specimen	Web Depth (in.)	Thickness (in.)	Area ($in.^2$)	Flange	Arc Length (in.)	Radius (in.)
50XF(39)CS3-2U	4.15	0.039	0.803	ATOP	3.18	1.01
				ABOT	3.20	1.02
				BTOP	3.17	1.02
				BBOT	3.15	1.00
30SKCS3-2B	3.95	0.029	0.606	ATOP	3.26	1.07
				ABOT	3.26	1.07
				BTOP	3.25	1.07
				BBOT	3.31	1.12
30SKCS3-3U	3.95	0.029	0.605	ATOP	3.37	1.08
				ABOT	3.32	1.07
				BTOP	3.29	1.09
				BBOT	3.39	1.08
80XFCS2-1B	3.70	0.085	1.50	ATOP	2.47	1.20
				ABOT	2.46	1.23
				BTOP	2.49	1.17
				BBOT	2.40	1.25
80XFCS2-3U	3.70	0.085	1.49	ATOP	2.44	1.21
				ABOT	2.49	1.25
				BTOP	2.49	1.22
				BBOT	2.46	1.23
50XF(78)CS2-1B	3.75	0.079	1.39	ATOP	2.41	1.27
				ABOT	2.44	1.27
				BTOP	2.36	1.27
				BBOT	2.46	1.16
50XF(78)CS2-2U	3.70	0.078	1.38	ATOP	2.46	1.22
				ABOT	2.38	1.21
				BTOP	2.52	1.25
				BBOT	2.38	1.20
80SKCS2-1B	3.80	0.062	1.09	ATOP	2.36	1.19
				ABOT	2.43	1.19
				BTOP	2.44	1.26
				BBOT	2.37	1.29
80SKCS2-2U	4.00	0.062	1.09	ATOP	2.43	1.24
				ABOT	2.34	1.24
				BTOP	2.36	1.30
				BBOT	2.40	1.27

Table 3.4 (Cont.)

Measured Dimensions of Stub Column Specimens

Specimen	Web Depth (in.)	Thickness (in.)	Area ($in.^2$)	Flange	Arc Length (in.)	Radius (in.)
80DKCS2-1B	3.75	0.047	0.830	ATOP	2.33	1.22
				ABOT	2.40	1.25
				BTOP	2.40	1.21
				BBOT	2.33	1.29
80DKCS2-2U	3.75	0.046	0.812	ATOP	2.41	1.17
				ABOT	2.34	1.16
				BTOP	2.35	1.18
				BBOT	2.46	1.19
50XF(39)CS2-1B	3.75	0.039	0.681	ATOP	2.47	1.14
				ABOT	2.45	1.18
				BTOP	2.56	1.19
				BBOT	2.32	1.13
50XF(39)CS2-2U	3.90	0.039	0.677	ATOP	2.26	1.16
				ABOT	2.37	1.23
				BTOP	2.40	1.22
				BBOT	2.41	1.20
30SKCS2-1B	3.70	0.029	0.512	ATOP	2.45	1.17
				ABOT	2.46	1.21
				BTOP	2.34	1.18
				BBOT	2.39	1.20
30SKCS2-2U	3.90	0.029	0.521	ATOP	2.39	1.15
				ABOT	2.38	1.13
				BTOP	2.40	1.15
				BBOT	2.37	1.15
80XFCS1-1U	3.65	0.085	1.40	ATOP	1.99	3.25
				ABOT	2.01	3.25
				BTOP	1.99	2.90
				BBOT	1.96	3.45
80XFCS1-2U	3.65	0.085	1.40	ATOP	2.00	2.85
				ABOT	2.00	3.35
				BTOP	1.99	3.05
				BBOT	2.02	3.25
50XF(78)CS1-1U	3.55	0.080	1.31	ATOP	2.04	3.35
				ABOT	1.97	4.25
				BTOP	2.05	3.25
				BBOT	2.04	4.05

Table 3.4 (Cont.)

Measured Dimensions of Stub Column Specimens

Specimen	Web Depth (in.)	Thickness (in.)	Area ($in.^2$)	Flange	Arc Length (in.)	Radius (in.)
50XF(78)CS1-2U	3.65	0.079	1.30	ATOP	1.98	4.45
				ABOT	2.06	3.40
				BTOP	2.05	3.55
				BBOT	2.04	3.35
80SKCS1-1U	3.45	0.062	1.02	ATOP	2.09	2.90
				ABOT	2.06	3.20
				BTOP	2.05	2.90
				BBOT	2.03	3.15
80SKCS1-2U	3.60	0.062	1.01	ATOP	2.02	3.25
				ABOT	2.09	3.15
				BTOP	2.05	3.20
				BBOT	1.96	3.30
80DKCS1-1U	3.45	0.047	0.768	ATOP	2.12	2.58
				ABOT	2.12	2.75
				BTOP	2.10	3.15
				BBOT	2.12	2.70
80DKCS1-2U	3.45	0.047	0.762	ATOP	2.09	2.50
				ABOT	2.03	2.70
				BTOP	2.00	2.90
				BBOT	2.09	2.53
50XF(39)CS1-2U	3.55	0.038	0.628	ATOP	1.97	3.90
				ABOT	2.09	3.05
				BTOP	1.98	2.75
				BBOT	2.05	3.10
50XF(39)CS1-3U	3.60	0.039	0.634	ATOP	2.08	3.50
				ABOT	1.97	3.90
				BTOP	2.04	3.45
				BBOT	2.04	3.20
30SKCS1-1U	3.55	0.029	0.476	ATOP	2.04	2.65
				ABOT	2.11	3.30
				BTOP	2.07	2.55
				BBOT	2.06	2.55
30SKCS1-2B	3.60	0.030	0.489	ATOP	2.03	2.95
				ABOT	2.05	2.90
				BTOP	1.97	2.80
				BBOT	1.97	3.35

Table 3.5

Parameters Used in Prediction of Curved Element Behavior

Initial Curved Element Failure

Specimen	First Flange	F_{pr}*	F_y*	$\frac{F_{pr}}{F_y}$	$\frac{R}{t}$	$\frac{b}{t}$
80XFCS3-1B	NONE	77.1	89.4	0.86	12.644	36.667
50XF(78)CS3-2B	ABOT	49.1	63.6	0.77	12.875	41.750
80SKCS3-2B	ABOT	53.0	75.4	0.70	17.097	54.032
80DKCS3-2B	NONE	45.9	54.1	0.85	23.478	68.913
50XF(39)CS3-3B	NONE	41.4	58.9	0.70	26.667	83.590
30SKCS3-2B	NONE	16.4	26.8	0.61	36.333	109.667
80XFCS2-1B	BBOT	77.1	89.4	0.86	14.706	28.235
50XF(78)CS2-1B	NONE	49.1	63.6	0.77	16.076	30.886
80SKCS2-1B	BTOP	53.0	75.4	0.70	20.323	39.355
80DKCS2-3B	ABOT	45.9	54.1	0.85	25.745	50.851
50XF(39)CS2-1B	BBOT	41.4	58.9	0.70	28.974	59.487
30SKCS2-1B	ABOT	16.4	26.8	0.61	41.724	84.828
80XFCS1-1U	ATOP	77.1	89.4	0.86	38.235	23.412
80XFCS1-2U	ABOT	77.1	89.4	0.86	39.412	23.529
50XF(78)CS1-1U	ABOT	49.1	63.6	0.77	53.125	24.625
50XF(78)CS1-2U	ATOP	49.1	63.6	0.77	56.329	25.063
80SKCS1-1U	BBOT	53.0	75.4	0.70	50.806	32.742
80SKCS1-2U	BTOP	53.0	75.4	0.70	51.613	33.065
80DKCS1-1U	BTOP	45.9	54.1	0.85	67.021	44.681
50XF(39)CS1-2U	ATOP	41.4	58.9	0.70	102.632	51.842
30SKCS1-2B	BTOP	16.4	26.8	0.61	93.333	65.6667

*Based on longitudinal compression tests.

Table 3.6

Comparison of Actual-to-Predicted Buckling Loads
Initial Curved Element Failure
(Based on Modified Redshaw's Eq. (3.5) Assuming
Elastic-Plastic Behavior, $F_{pr} = F_y$)

Specimen	Ultimate Load (kips) (1)	Initial Buckling Load (kips) (2)	Predicted Buckling Load (kips) (3)	(2)/(3) (4)	(1)/(3) (5)	(1)/(2) (6)
80XFCS3-1B*	135.0	135.0	163.0	0.83	0.83	1.00
50XF(78)CS3-3B*	93.7	92.8	106.0	0.88	0.88	1.01
80SKCS3-2B	85.6	84.4	86.5	0.98	0.99	1.01
80DKCS3-2B	45.8	45.8	46.8	0.98	0.98	1.00
50XF(39)CS3-3B	32.0	32.0	34.5	0.93	0.93	1.00
30SKCS3-2B*	14.3	14.3	16.2	0.88	0.88	1.00
80XFCS2-1B	120.0	117.0	126.0	0.93	0.95	1.03
50XF(78)CS2-1B*	75.0	74.5	88.2	0.84	0.85	1.01
80SKCS2-1B	62.6	57.0	64.2	0.89	0.97	1.10
80DKCS2-3B	39.9	39.8	37.7	1.06	1.06	1.00
50XF(39)CS2-1B	28.0	27.4	27.3	1.00	1.03	1.02
30SKCS2-1B*	10.8	10.4	13.7	0.76	0.79	1.04
80XFCS1-1U	78.2	73.7	61.0	1.20	1.28	1.06
80XFCS1-2U	78.3	77.7	60.0	1.30	1.31	1.01
50XF(78)CS1-1U	57.0	48.8	45.2	1.08	1.26	1.17
50XF(78)CS1-2U	54.4	49.5	42.8	1.16	1.27	1.10
80SKCS1-1U	41.5	34.3	29.4	1.17	1.41	1.21
80SKCS1-2U	39.8	33.8	28.7	1.18	1.39	1.18
80DKCS1-1U	25.2	22.4	15.5	1.45	1.63	1.13
50XF(39)CS1-2U	15.7	11.8	8.50	1.39	1.85	1.33
30SKCS1-2B	9.38	7.88	6.60	1.19	1.42	1.19
Mean				1.05	1.14	
Std. Deviation				0.191	0.287	

*$f_{cr} > F_y$; use $f_{cr} = F_y$

Table 3.7

Comparison of Actual-to-Predicted Buckling Loads
Initial Curved Element Failure
(Based on Modified Redshaw's Eq. (3.5) with $E = E_t$
Using F_y and F_{pr} of Each Material)

Specimen	Ultimate Load (kips) (1)	Initial Buckling Load (kips) (2)	Predicted Buckling Load (kips) (3)	(2)/(3) (4)	(1)/(3) (5)
80XFCS3-1B*	135.0	135.0	144.3	0.94	0.94
50XF(78)CS3-3B*	93.7	92.8	92.8	1.00	1.01
80SKCS3-2B*	85.6	84.4	74.5	1.13	1.15
80DKCS3-2B*	45.8	45.8	44.6	1.03	1.03
50XF(39)CS3-3B*	32.0	32.0	34.0	0.94	0.94
30SKCS3-2B*	14.3	14.3	12.9	1.11	1.11
80XFCS2-1B*	120.0	117.0	117.3	1.00	1.02
50XF(78)CS2-1B*	75.0	74.5	75.7	0.98	0.99
80SKCS2-1B*	62.6	57.0	60.3	0.95	1.04
80DKCS2-3B	39.9	39.8	37.7	1.06	1.06
50XF(39)CS2-1B	28.0	27.4	27.3	1.00	1.03
30SKCS2-1B*	10.8	10.4	10.6	0.98	1.02
80XFCS1-1U	78.2	73.7	61.0	1.21	1.28
80XFCS1-2U	78.3	77.7	59.6	1.30	1.31
50XF(78)CS1-1U	57.0	48.8	45.2	1.08	1.26
50XF(78)CS1-2U	54.4	49.5	42.8	1.16	1.27
80SKCS1-1U	41.5	34.3	29.4	1.17	1.41
80SKCS1-2U	39.8	33.8	28.7	1.18	1.39
80DKCS1-1U	25.2	22.4	15.5	1.45	1.63
50XF(39)CS1-2U	15.7	11.8	8.50	1.39	1.85
30SKCS1-2B	9.38	7.88	6.60	1.19	1.42
Mean				1.11	1.20
Std. Deviation				0.145	0.240

*$f_{cr} > F_{pr}$.

Table 3.8

Comparison of Actual-to-Predicted Buckling Loads
Initial Curved Element Failure
(Based on Modified Redshaw's Eq. (3.5) with $E = E_t$
Using $F_{pr} = 0.7*F_y$ of Each Material)

Specimen	Ultimate Load (kips) (1)	Initial Buckling Load (kips) (2)	Predicted Buckling Load (kips) (3)	(2)/(3) (4)	(1)/(3) (5)
80XFCS3-1B*	135.0	135.0	130.1	1.04	1.04
50XF(78)CS3-3B*	93.7	92.8	90.2	1.03	1.03
80SKCS3-2B*	85.6	84.4	74.3	1.13	1.15
80DKCS3-2B*	45.8	45.8	39.9	1.15	1.15
50XF(39)CS3-3B*	32.0	32.0	33.9	0.94	0.94
30SKCS3-2B*	14.3	14.3	13.3	1.07	1.07
80XFCS2-1B*	120.0	117.0	104.2	1.12	1.15
50XF(78)CS2-1B*	75.0	74.5	72.8	1.02	1.03
80SKCS2-1B*	62.6	57.0	60.1	0.95	1.04
80DKCS2-3B*	39.9	39.8	33.6	1.18	1.19
50XF(39)CS2-1B	28.0	27.4	27.3	1.00	1.03
30SKCS2-1B*	10.8	10.4	10.9	0.95	0.99
80XFCS1-1U	78.2	73.7	61.0	1.21	1.28
80XFCS1-2U	78.3	77.7	59.6	1.30	1.31
50XF(78)CS1-1U	57.0	48.8	45.2	1.08	1.26
50XF(78)CS1-2U	54.4	49.5	42.8	1.16	1.27
80SKCS1-1U	41.5	34.3	29.4	1.16	1.41
80SKCS1-2U	39.8	33.8	28.7	1.18	1.39
80DKCS1-1U	25.2	22.4	15.5	1.45	1.63
50XF(39)CS1-2U	15.7	11.8	8.50	1.39	1.85
30SKCS1-2B	9.38	7.88	6.60	1.19	1.42
Mean				1.13	1.22
Std. Deviation				0.136	0.226

*$f_{cr} > F_{pr}$

Table 3.9

Comparison of Actual-to-Predicted Buckling Loads
Initial Curved Element Failure
(Based on Regression Eq. (3.5a) Assuming
Elastic-Plastic Behavior, $F_{pr} = F_y$)

Specimen	Ultimate Load (kips) (1)	Initial Buckling Load (kips) (2)	Predicted Buckling Load (kips) (3)	(2)/(3) (4)	(1)/(3) (5)
80XFCS3-1B	135.0	135.0	155.1	0.87	0.87
50XF(78)CS3-3B*	93.7	92.8	106.0	0.88	0.88
80SKCS3-2B	85.6	84.4	79.9	1.06	1.07
80DKCS3-2B	45.8	45.8	44.1	1.04	1.04
50XF(39)CS3-3B	32.0	32.0	32.3	0.99	0.99
30SKCS3-2B*	14.3	14.3	16.2	0.88	0.88
80XFCS2-1B	120.0	117.0	120.8	0.97	0.99
50XF(78)CS2-1B*	75.0	74.5	88.2	0.84	0.85
80SKCS2-1B	62.6	57.0	63.4	0.90	0.99
80DKCS2-3B	39.9	39.8	37.7	1.06	1.06
50XF(39)CS2-1B	28.0	27.4	27.3	1.00	1.02
30SKCS2-1B*	10.8	10.4	13.7	0.76	0.79
80XFCS1-1U	78.2	73.7	68.5	1.08	1.14
80XFCS1-2U	78.3	77.7	67.4	1.15	1.16
50XF(78)CS1-1U	57.0	48.8	54.1	0.90	1.05
50XF(78)CS1-2U	54.4	49.5	51.9	0.95	1.05
80SKCS1-1U	41.5	34.3	36.5	0.94	1.14
80SKCS1-2U	39.8	33.8	35.7	0.95	1.11
80DKCS1-1U	25.2	22.4	20.5	1.09	1.23
50XF(39)CS1-2U	15.7	11.8	12.8	0.93	1.23
30SKCS1-2B	9.38	7.88	9.11	0.86	1.03
Mean				0.96	1.03
Std. Deviation				0.097	0.122

*$f_{cr} > F_y$; use $f_{cr} = F_y$

Table 3.10

Comparison of Actual-to-Predicted Buckling Loads
Initial Curved Element Failure
(Based on Regression Eq. (3.5a) with $E = E_t$
Using F_y and F_{pr} of Each Material)

Specimen	Ultimate Load (kips) (1)	Initial Buckling Load (kips) (2)	Predicted Buckling Load (kips) (3)	(2)/(3) (4)	(1)/(3) (5)
80XFCS3-1B*	135.0	135.0	142.7	0.95	0.95
50XF(78)CS3-3B*	93.7	92.8	91.6	1.01	1.02
80SKCS3-2B*	85.6	84.4	72.5	1.16	1.18
80DKCS3-2B	45.8	45.8	44.1	1.04	1.04
50XF(39)CS3-3B	32.0	32.0	32.3	0.99	0.99
30SKCS3-2B*	14.3	14.3	12.8	1.12	1.12
80XFCS2-1B*	120.0	117.0	116.4	1.01	1.03
50XF(78)CS2-1B*	75.0	74.5	74.8	1.00	1.00
80SKCS2-1B*	62.6	57.0	60.0	0.95	1.04
80DKCS2-3B	39.9	39.8	37.7	1.06	1.06
50XF(39)CS2-1B	28.0	27.4	27.3	1.00	1.02
30SKCS2-1B*	10.8	10.4	10.6	0.98	1.02
80XFCS1-1U	78.2	73.7	68.5	1.08	1.14
80XFCS1-2U	78.3	77.7	67.4	1.15	1.16
50XF(78)CS1-1U	57.0	48.8	54.1	0.90	1.05
50XF(78)CS1-2U	54.4	49.5	51.9	0.95	1.05
80SKCS1-1U	41.5	34.3	36.5	0.94	1.14
80SKCS1-2U	39.8	33.8	35.7	0.95	1.11
80DKCS1 1U	25.2	22.4	20.5	1.09	1.23
50XF(39)CS1-2U	15.7	11.8	12.8	0.93	1.23
30SKCS1-2B*	9.38	7.88	8.64	0.91	1.09
Mean				1.01	1.08
Std. Deviation				0.078	0.078

*$f_{cr} > F_{pr}$.

Table 3.11

Comparison of Actual-to-Predicted Buckling Loads
Initial Curved Element Failure
(Based on Regression Eq. (3.5a) with $E = E_t$
Using $F_{pr} = 0.7*F_y$ of Each Material)

Specimen	Ultimate Load (kips) (1)	Initial Buckling Load (kips) (2)	Predicted Buckling Load (kips) (3)	(2)/(3) (4)	(1)/(3) (5)
80XFCS3-1B*	135.0	135.0	127.1	1.06	1.06
50XF(78)CS3-3B*	93.7	92.8	88.6	1.05	1.05
80SKCS3-2B*	85.6	84.4	72.5	1.16	1.18
80DKCS3-2B*	45.8	45.8	39.2	1.17	1.17
50XF(39)CS3-3B	32.0	32.0	32.3	0.99	0.99
30SKCS3-2B*	14.3	14.3	13.1	1.09	1.09
80XFCS2-1B*	120.0	117.0	102.8	1.14	1.17
50XF(78)CS2-1B*	75.0	74.5	72.1	1.03	1.04
80SKCS2-1B*	62.6	57.0	59.8	0.95	1.05
80DKCS2-3B*	39.9	39.8	33.6	1.18	1.19
50XF(39)CS2-1B	28.0	27.4	27.3	1.00	1.02
30SKCS2-1B*	10.8	10.4	11.0	0.95	0.98
80XFCS1-1U	78.2	73.7	68.5	1.08	1.14
80XFCS1-2U	78.3	77.7	67.4	1.15	1.16
50XF(78)CS1-1U	57.0	48.8	54.1	0.90	1.05
50XF(78)CS1-2U	54.4	49.5	51.9	0.95	1.05
80SKCS1-1U	41.5	34.3	36.5	0.94	1.14
80SKCS1-2U	39.8	33.8	35.7	0.95	1.11
80DKCS1-1U	25.2	22.4	20.5	1.09	1.23
50XF(39)CS1-2U	15.7	11.8	12.8	0.93	1.23
30SKCS1-2B	9.38	7.88	9.11	0.86	1.03
Mean				1.03	1.10
Std. Deviation				0.098	0.076

*$f_{cr} > F_{pr}$

Table 3.12

Summary of Initial Buckling-to-Predicted Load Ratios
for Tables 3.6 Thru 3.11
Initial Curved Element Failure

	Table 3.6	3.7	3.8	3.9	3.10	3.11
80XFC3-1B	0.83	0.94	1.04	0.87	0.95	1.06
50XF(78)C3-2B	0.88	1.00	1.03	0.88	1.01	1.05
80SKC3-2B	0.98	1.13	1.13	1.06	1.16	1.16
80DKC3-2B	0.98	1.03	1.15	1.04	1.04	1.17
50XF(39)C3-3B	0.93	0.94	0.94	0.99	0.99	0.99
30SKC3-2B	0.88	1.11	1.07	0.88	1.12	1.09
80XFC2-1B	0.93	1.00	1.12	0.97	1.01	1.14
50XF(78)C2-1B	0.84	0.98	1.02	0.84	1.00	1.03
80SKC2-1B	0.89	0.95	0.95	0.90	0.95	0.95
80DKC2-3B	1.06	1.06	1.18	1.06	1.06	1.18
50XF(39)C2-1B	1.00	1.00	1.00	1.00	1.00	1.00
30SKC2-1B	0.76	0.98	0.95	0.76	0.98	0.95
80XFC1-1U	1.20	1.21	1.21	1.08	1.08	1.08
80XFC1-2U	1.30	1.30	1.30	1.15	1.15	1.15
50XF(78)C1-1U	1.08	1.08	1.08	0.90	0.90	0.90
50XF(78)C1-2U	1.16	1.16	1.16	0.95	0.95	0.95
80SKC1-1U	1.17	1.17	1.16	0.94	0.94	0.94
80SKC1-2U	1.18	1.18	1.18	0.95	0.95	0.95
80DKC1-1U	1.45	1.45	1.45	1.09	1.09	1.09
50XF(39)C1-2U	1.39	1.39	1.39	0.93	0.93	0.93
30SKC1-2B	1.19	1.19	1.19	0.86	0.91	0.86
Mean	1.05	1.11	1.13	0.96	1.01	1.03
Std. Deviation	0.191	0.145	0.136	0.097	0.078	0.098

Table 3.13

Summary of Ultimate-to-Predicted Load Ratios
for Tables 3.6 Thru 3.11
Initial Curved Element Failure

	Table					
	3.6	3.7	3.8	3.9	3.10	3.11
80XFC3-1B	0.83	0.94	1.04	0.87	0.95	1.06
50XF(78)C3-2B	0.88	1.01	1.03	0.88	1.02	1.05
80SKC3-2B	0.99	1.15	1.15	1.07	1.18	1.18
80DKC3-2B	0.98	1.03	1.15	1.04	1.04	1.17
50XF(39)C3-3B	0.93	0.94	0.94	0.99	0.99	0.99
30SKC3-2B	0.88	1.11	1.07	0.88	1.12	1.09
80XFC2-1B	0.95	1.02	1.15	0.99	1.03	1.17
50XF(78)C2-1B	0.85	0.99	1.03	0.85	1.00	1.04
80SKC2-1B	0.97	1.04	0.04	0.99	1.04	1.05
80DKC2-3B	1.06	1.06	1.19	1.06	1.06	1.19
50XF(39)C2-1B	1.03	1.03	1.03	1.02	1.02	1.02
30SKC2-1B	0.79	1.02	0.99	0.79	1.02	0.98
80XFC1-1U	1.28	1.28	1.28	1.14	1.14	1.14
80XFC1-2U	1.31	1.31	1.31	1.16	1.16	1.16
50XF(78)C1-1U	1.26	1.26	1.26	1.05	1.05	1.05
50XF(78)C1-2U	1.27	1.27	1.27	1.05	1.05	1.05
80SKC1-1U	1.41	1.41	1.41	1.14	1.14	1.14
80SKC1-2U	1.39	1.39	1.39	1.11	1.11	1.11
80DKC1-1U	1.63	1.63	1.63	1.23	1.23	1.23
50XF(39)C1-2U	1.85	1.85	1.85	1.23	1.23	1.23
30SKC1-2B	1.42	1.42	1.42	1.03	1.09	1.03
Mean	1.14	1.20	1.22	1.03	1.08	1.10
Std. Deviation	0.287	0.240	0.226	0.122	0.078	0.076

Table 3.14

Parameters Used in Prediction of Curved Element Behavior

Initial Flat Element Failure

Specimen	First Flange	F_{pr}^{*}	F_{y}^{*}	$\frac{F_{pr}}{Fy}$	$\frac{R}{t}$	$\frac{b}{t}$
80XFCS3-2U	ATOP	77.1	89.4	0.86	12.759	37.126
50XF(78)CS3-1U	NONE	49.1	63.6	0.77	13.165	40.886
80SKCS3-3U	ATOP	53.0	75.4	0.70	17.705	52.131
80DKCS3-3U	NONE	45.9	54.1	0.85	23.830	69.149
50XF(39)CS3-2U	NONE	41.4	58.9	0.70	26.425	82.902
30SKCS3-3U	NONE	16.4	26.8	0.61	37.586	113.448
80XFCS2-3U	ABOT	77.1	89.4	0.86	14.706	29.294
50XF(78)CS2-2U	NONE	49.1	63.6	0.77	16.026	32.308
80SKCS2-2U	NONE	53.0	75.4	0.70	21.002	38.126
80DKCS2-2U	ATOP	45.9	54.1	0.85	25.270	52.052
50XF(39)CS2-2U	ABOT	41.4	58.9	0.70	31.783	61.240
30SKCS2-2U	ATOP	16.4	26.8	0.61	38.983	81.017
80DKCS1-2U	ABOT	45.9	54.1	0.85	58.065	43.656
50XF(39)CS1-3U	BTOP	41.4	58.9	0.70	88.462	52.308
30SKCS1-1U	ABOT	16.4	26.8	0.61	113.793	72.759

*Based on longitudinal compression tests.

Table 3.15

Comparison of Actual-to-Predicted Buckling Loads
Initial Flat Element Failure
(P_{curve} Based on Modified Redshaw's Eq. (3.5)
Assuming Elastic-Plastic Behavior, $F_{pr} = F_y$)

Specimen	Ultimate Load (kips) (1)	Initial Buckling Load (kips) (2)	P_w (kips) (3)	P_{curve} (kips) (4)	P_{total} (kips) (5)	(2)/(5) (6)	(1)/(5) (7)
80XFCS3-2U*	111.2	110.0	63.5	97.8	161.3	0.68	0.69
50XF(78)CS3-1U*	70.0	70.0	42.2	62.1	104.3	0.67	0.67
80SKCS3-3U	74.6	72.1	29.1	49.8	78.9	0.91	0.95
80DKCS3-3U	39.0	39.0	15.2	28.2	43.4	0.90	0.90
50XF(39)CS3-2U	32.0	32.0	10.1	20.7	30.8	1.04	1.04
30SKCS3-3U*	11.9	11.9	4.53	10.1	14.6	0.81	0.81
80XFCS2-3U	101.6	101.3	52.5	72.2	124.7	0.81	0.81
50XF(78)CS2-2U*	62.6	62.6	36.7	51.0	87.7	0.71	0.71
80SKCS2-2U	57.7	56.4	26.9	34.0	60.9	0.93	0.95
80DKCS2-2U	32.7	32.7	14.1	21.5	35.6	0.92	0.92
50XF(39)CS2-2U	23.3	20.3	9.06	13.7	22.8	0.89	1.02
30SKCS2-2U*	9.43	9.20	4.65	7.80	12.5	0.74	0.76
80DKCS1-2U	22.5	21.5	7.35	10.1	17.4	1.23	1.29
50XF(39)CS1-3U	14.0	11.3	4.26	5.36	9.62	1.17	1.46
30SKCS1-1U	7.05	4.90	2.29	3.00	5.29	0.93**	1.34**
Mean						0.89	0.93
Std. Deviation						0.172	0.225

*$f_{cr} > F_y$; use $f_{cr} = F_y$ for P_{curve}

**Not included in the calculation of mean and standard deviation.

P_w = predicted web strength based on predicted curved element buckling stress at edges of web

P_{curve} = predicted curved element buckling load

P_{total} = predicted total load that section can withstand
= $P_w + P_{curve}$

Table 3.16

Comparison of Actual-to-Predicted Buckling Loads
Initial Flat Element Failure
(P_{curve} Based on Modified Redshaw's Eq. (3.5) with $E = E_t$
Using F_y and F_{pr} of Each Material)

Specimen	Ultimate Load (kips) (1)	Initial Buckling Load (kips) (2)	P_w (kips) (3)	P_{curve} (kips) (4)	P_{total} (kips) (5)	(2)/(5) (6)	(1)/(5) (7)
80XFCS3-2U*	111.2	110.0	56.4	86.5	143.0	0.77	0.78
50XF(78)CS3-1U*	70.0	70.0	36.8	54.2	91.1	0.77	0.77
80SKCS3-3U*	74.6	72.1	26.6	43.8	70.4	1.02	1.06
80DKCS3-3U*	39.0	39.0	14.9	27.3	42.2	0.92	0.92
50XF(39)CS3-2U*	32.0	32.0	10.0	20.3	30.3	1.06	1.06
30SKCS3-3U*	11.9	11.9	3.90	7.98	11.9	1.00	1.00
80XFCS2-3U*	101.6	101.3	49.1	67.6	116.6	0.87	0.87
50XF(78)CS2-2U*	62.6	62.6	31.3	43.5	74.8	0.84	0.84
80SKCS2-2U*	57.7	56.4	26.0	32.4	58.3	0.97	0.99
80DKCS2-2U*	32.7	32.7	14.0	21.4	35.4	0.92	0.92
50XF(39)CS2-2U	23.3	20.3	9.06	13.7	22.8	0.89	1.02
30SKCS2-2U*	9.43	9.20	3.98	6.13	10.1	0.91	0.93
80DKCS1-2U	22.5	21.5	7.34	10.1	17.4	1.23	1.29
50XF(39)CS1-3U	14.0	11.3	4.26	5.36	9.62	1.17	1.46
30SKCS1-1U	7.05	4.90	2.28	2.99	5.27	0.93**	1.34**
Mean						0.95	0.99
Std. Deviation						0.136	0.188

*$f_{cr} > F_{pr}$ for curved element

**Not included in calculation of mean and standard deviation.

P_w = predicted web strength based on predicted curved element buckling stress at edges of web

P_{curve} = predicted curved element buckling load

P_{total} = predicted total load that section can withstand
$= P_w + P_{curve}$

Table 3.17

Comparison of Actual-to-Predicted Buckling Loads
Initial Flat Element Failure
(P_{curve} Based on Modified Redshaw's Eq. (3.5) with $E = E_t$
Using $F_{pr} = 0.7*F_y$ of Each Material)

Specimen	Ultimate Load (kips) (1)	Initial Buckling Load (kips) (2)	P_w (kips) (3)	P_{curve} (kips) (4)	P_{total} (kips) (5)	(2)/(5) (6)	(1)/(5) (7)
80XFCS3-2U*	111.2	110.0	50.8	77.8	128.6	0.86	0.86
50XF(78)CS3-1U*	70.0	70.0	35.8	52.7	88.6	0.79	0.79
80SKCS3-3U*	74.6	72.1	26.6	43.8	70.4	1.02	1.06
80DKCS3-3U*	39.0	39.0	13.8	24.3	38.1	1.02	1.02
50XF(39)CS3-2U*	32.0	32.0	10.0	20.2	30.2	1.06	1.06
30SKCS3-3U*	11.9	11.9	3.96	8.19	12.2	0.97	0.98
80XFCS2-3U*	101.6	101.3	43.6	60.0	103.7	0.98	0.98
50XF(78)CS2-2U*	62.6	62.6	30.2	42.0	72.2	0.87	0.87
80SKCS2-2U*	57.7	56.4	25.9	32.3	58.2	0.97	0.99
80DKCS2-2U*	32.7	32.7	12.9	19.0	31.9	1.02	1.02
50XF(39)CS2-2U	23.3	20.3	9.06	13.7	22.8	0.89	1.02
30SKCS2-2U*	9.43	9.20	4.05	6.29	10.3	0.89	0.91
80DKCS1-2U	22.5	21.5	7.34	10.1	17.4	1.23	1.29
50XF(39)CS1-3U	14.0	11.3	4.26	5.36	9.62	1.17	1.45
30SKCS1-1U	7.05	4.90	2.28	2.99	5.27	0.93**	1.34**
Mean						0.98	1.02
Std. Deviation						0.122	0.171

*$f_{cr} > F_{pr}$

**Not included in calculation of mean and standard deviation.

P_w = predicted web strength based on predicted curved element buckling stress at edges of web

P_{curve} = predicted curved element buckling load

P_{total} = predicted total load that section can withstand
$= P_w + P_{curve}$

Table 3.18

Comparison of Actual-to-Predicted Buckling Loads
Initial Flat Element Failure
(P_{curve} Based on Regression Eq. (3.5a)
Assuming Elastic-Plastic Behavior, $F_{pr} = F_y$)

Specimen	Ultimate Load (kips) (1)	Initial Buckling Load (kips) (2)	P_w (kips) (3)	P_{curve} (kips) (4)	P_{total} (kips) (5)	(2)/(5) (6)	(1)/(5) (7)
80XFCS3-2U	111.2	110.0	60.1	92.2	152.3	0.72	0.73
50XF(78)CS3-1U*	70.0	70.0	42.2	62.1	104.3	0.67	0.67
80SKCS3-3U	74.6	72.1	27.7	46.4	74.1	0.97	1.01
80DKCS3-3U	39.0	39.0	14.6	26.6	41.2	0.95	0.95
50XF(39)CS3-2U	32.0	32.0	9.73	19.4	29.1	1.10	1.10
30SKCS3-3U*	11.9	11.9	4.53	10.1	14.6	0.81	0.81
80XFCS2-3U	101.6	101.3	50.2	69.1	119.3	0.85	0.85
50XF(78)CS2-2U*	62.6	62.6	36.7	51.0	87.7	0.71	0.71
80SKCS2-2U	57.7	56.4	26.8	33.8	60.6	0.93	0.95
80DKCS2-2U	32.7	32.7	14.0	21.4	35.4	0.92	0.92
50XF(39)CS2-2U	23.3	20.3	9.15	14.0	23.2	0.88	1.01
30SKCS2-2U*	9.43	9.20	4.65	7.80	12.5	0.74	0.76
80DKCS1-2U	22.5	21.5	9.30	12.8	22.1	0.97	1.02
50XF(39)CS1-3U	14.0	11.3	6.05	7.61	13.6	0.82	1.02
30SKCS1-1U	7.05	4.90	3.12	4.34	7.46	0.66**	0.95**
Mean						0.86	0.89
Std. Deviation						0.123	0.137

*$f_{cr} > F_y$; use $f_{cr} = F_y$

**Not included in the calculation of mean and standard deviation.

P_w = predicted web strength based on predicted curved element buckling stress at edges of web

P_{curve} = predicted curved element buckling load

P_{total} = predicted total load that section can withstand
$= P_w + P_{curve}$

Table 3.19

Comparison of Actual-to-Predicted Buckling Loads
Initial Flat Element Failure
(P_{curve} Based on Regression Eq. (3.5a) with $E = E_t$
Using F_y and F_{pr} of Each Material)

Specimen	Ultimate Load (kips) (1)	Initial Buckling Load (kips) (2)	P_w (kips) (3)	P_{curve} (kips) (4)	P_{total} (kips) (5)	(2)/(5) (6)	(1)/(5) (7)
80XFCS3-2U*	111.2	110.0	55.8	85.5	141.3	0.78	0.79
50XF(78)CS3-1U*	70.0	70.0	36.3	53.4	89.7	0.78	0.78
80SKCS3-3U*	74.6	72.1	26.2	42.7	68.9	1.05	1.08
80DKCS3-3U	39.0	39.0	14.6	26.6	41.3	0.95	0.95
50XF(39)CS3-2U	32.0	32.0	9.73	19.4	29.1	1.10	1.10
30SKCS3-3U*	11.9	11.9	3.86	7.86	11.7	1.01	1.02
80XFCS2-3U*	101.6	101.3	48.7	67.1	115.8	0.87	0.88
50XF(78)CS2-2U*	62.6	62.6	31.1	43.2	74.3	0.84	0.84
80SKCS2-2U*	57.7	56.4	25.9	32.3	58.3	0.97	0.99
80DKCS2-2U*	32.7	32.7	14.0	21.4	35.4	0.92	0.92
50XF(39)CS2-2U	23.3	20.3	9.15	14.0	23.2	0.88	1.01
30SKCS2-2U*	9.43	9.20	3.99	6.15	10.1	0.91	0.93
80DKCS1-2U	22.5	21.5	9.30	12.8	22.1	0.97	1.02
50XF(39)CS1-3U	14.0	11.3	6.05	7.61	13.7	0.82	1.02
30SKCS1-1U	7.05	4.90	3.12	4.34	7.46	0.66**	0.95**
Mean						0.92	0.95
Std. Deviation						0.097	0.101

*$f_{cr} > F_{pr}$ for curved elements

**Not included in calculation of mean and standard deviation.

P_w = predicted web strength based on predicted curved element buckling stress at edges of web

P_{curve} = predicted curved element buckling load

P_{total} = predicted total load that section can withstand
$= P_w + P_{curve}$

Table 3.20

Comparison of Actual-to-Predicted Buckling Loads
Initial Flat Element Failure
(P_{curve} Based on Regression Eq. (3.5a) with $E = E_t$
Using $F_{pr} = 0.7*F_y$ of Each Material)

Specimen	Ultimate Load (kips) (1)	Initial Buckling Load (kips) (2)	P_w (kips) (3)	P_{curve} (kips) (4)	P_{total} (kips) (5)	(2)/(5) (6)	(1)/(5) (7)
80XFCS3-2U*	111.2	110.0	49.6	76.1	125.7	0.88	0.88
50XF(78)CS3-1U*	70.0	70.0	35.2	51.8	87.0	0.80	0.80
80SKCS3-3U*	74.6	72.1	26.1	42.7	68.8	1.05	1.08
80DKCS3-3U*	39.0	39.0	13.6	23.9	37.5	1.04	1.04
50XF(39)CS3-2U	32.0	32.0	9.73	19.4	29.1	1.10	1.10
30SKCS3-3U*	11.9	11.9	3.94	8.13	12.1	0.98	0.99
80XFCS2-3U*	101.6	101.3	43.0	59.2	102.3	0.99	0.99
50XF(78)CS2-2U*	62.6	62.6	30.0	41.6	71.6	0.87	0.87
80SKCS2-2U*	57.7	56.4	25.9	32.3	58.2	0.97	0.99
80DKCS2-2U*	32.7	32.7	12.9	19.0	31.9	1.03	1.03
50XF(39)CS2-2U	23.3	20.3	9.15	14.0	23.2	0.88	1.01
30SKCS2-2U*	9.43	9.20	4.07	6.34	10.4	0.88	0.91
80DKCS1-2U	22.5	21.5	9.30	12.8	22.1	0.97	1.02
50XF(39)CS1-3U	14.0	11.3	6.05	7.61	13.6	0.82	1.02
30SKCS1-1U	7.05	4.90	3.12	4.34	7.46	0.66**	0.95**
Mean						0.95	0.98
Std. Deviation						0.091	0.084

* $f_{cr} > F_{pr}$ for curved element

** Not included in calculation of mean and standard deviation.

P_w = predicted web strength based on predicted curved element buckling stress at edges of web

P_{curve} = predicted curved element buckling load

P_{total} = predicted total load that section can withstand
$= P_w + P_{curve}$

Table 3.21

Summary of Initial Buckling-to-Predicted Load Ratios
for Tables 3.15 Thru 3.20
Initial Flat Element Failure

	Table					
	3.15	3.16	3.17	3.18	3.19	3.20
80XFC3-2U	0.68	0.77	0.86	0.72	0.78	0.88
50XF(78)C3-1U	0.67	0.77	0.79	0.67	0.78	0.80
80SKC3-3U	0.91	1.02	1.02	0.97	1.05	1.05
80DKC3-3U	0.90	0.92	1.02	0.95	0.95	1.04
50XF(39)C3-2U	1.04	1.06	1.06	1.10	1.10	1.10
30SKC3-3U	0.81	1.00	0.97	0.81	1.01	0.98
80XFC2-3U	0.81	0.87	0.98	0.85	0.87	0.99
50XF(78)C2-2U	0.71	0.84	0.87	0.71	0.84	0.87
80SKC2-2U	0.93	0.97	0.97	0.93	0.97	0.97
80DKC2-2U	0.92	0.92	1.02	0.92	0.92	1.03
50XF(39)C2-2U	0.89	0.89	0.89	0.88	0.88	0.88
30SKC2-2U	0.74	0.91	0.89	0.74	0.91	0.88
80DKC1-2U	1.23	1.23	1.23	0.97	0.97	0.97
50XF(39)C1-3U	1.17	1.17	1.17	0.82	0.82	0.82
30SKC1-1U*	0.93	0.93	0.93	0.66	0.66	0.66
Mean	0.89	0.95	0.98	0.86	0.92	0.95
Std. Deviation	0.172	0.136	0.122	0.123	0.097	0.091

*Not included in the calculation of mean and standard deviation.

Table 3.22

Summary of Ultimate-to-Predicted Load Ratios
for Tables 3.15 Thru 3.20
Initial Flat Element Failure

	Table					
	3.15	3.16	3.17	3.18	3.19	3.20
80XFC3-2U	0.69	0.78	0.86	0.73	0.79	0.88
50XF(78)C3-1U	0.67	0.77	0.79	0.67	0.78	0.80
80SKC3-3U	0.95	1.06	1.06	1.01	1.08	1.08
80DKC3-3U	0.90	0.92	1.02	0.95	0.95	1.04
50XF(39)C3-2U	1.04	1.06	1.06	1.10	1.10	1.10
30SKC3-3U	0.81	1.00	0.98	0.81	1.02	0.99
80XFC2-3U	0.81	0.87	0.98	0.85	0.88	0.99
50XF(78)C2-2U	0.71	0.84	0.87	0.71	0.84	0.87
80SKC2-2U	0.95	0.99	0.99	0.95	0.99	0.99
80DKC2-2U	0.92	0.92	1.02	0.92	0.92	1.03
50XF(39)C2-2U	1.02	1.02	1.02	1.01	1.01	1.01
30SKC2-2U	0.76	0.93	0.91	0.76	0.93	0.91
80DKC1-2U	1.29	1.29	1.29	1.02	1.02	1.02
50XF(39)C1-3U	1.46	1.46	1.45	1.02	1.02	1.02
30SKC1-1U*	1.34	1.34	1.34	0.95	0.95	0.95
Mean	0.93	0.99	1.02	0.89	0.95	0.98
Std. Deviation	0.225	0.188	0.171	0.137	0.101	0.084

*Not included in the calculation of mean and standard deviation.

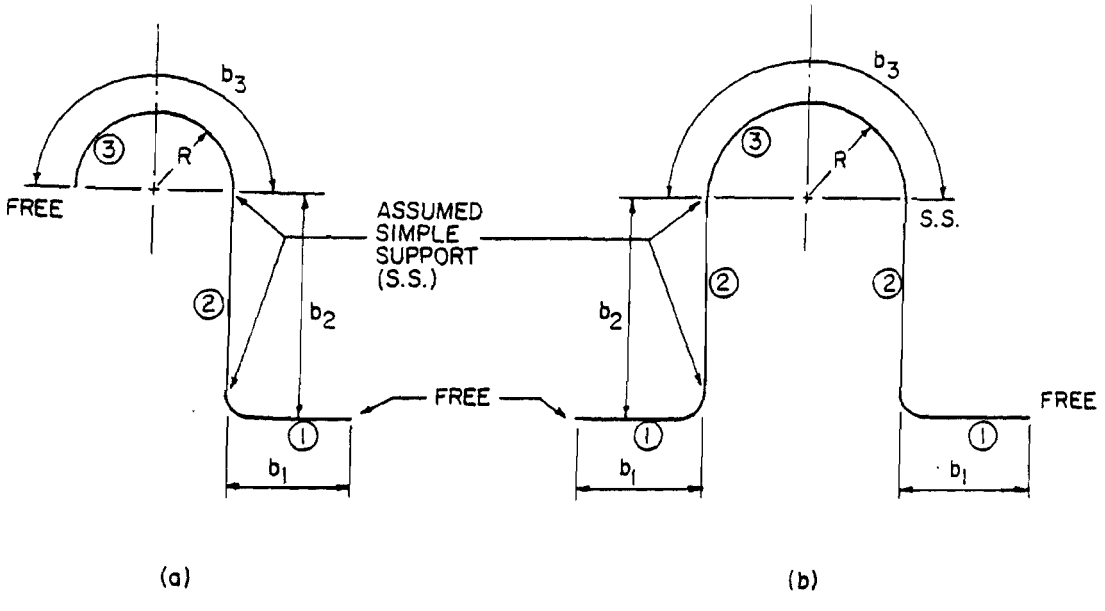

Fig. 3.1 Typical Cross Sections Consisting of Flat and Curved Elements

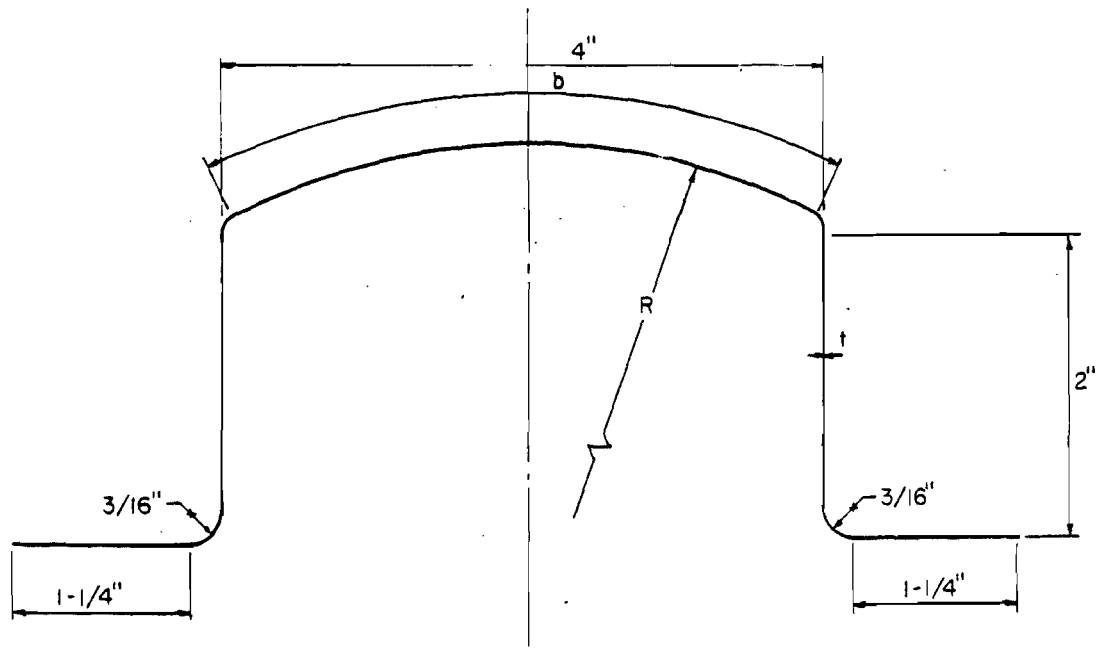

Fig. 3.2 A Profile

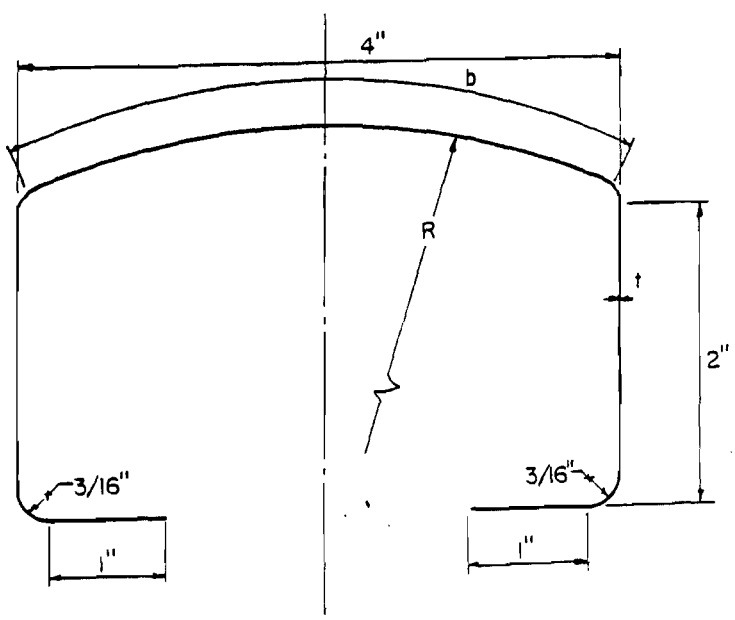

Fig. 3.3 B Profile

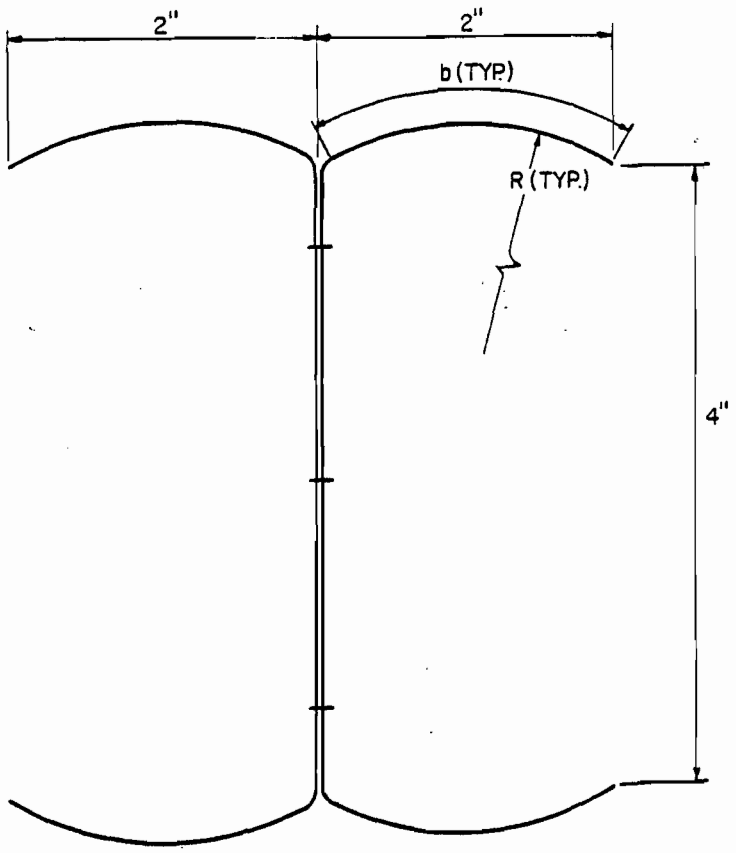

Fig. 3.4 CS and CB Profile

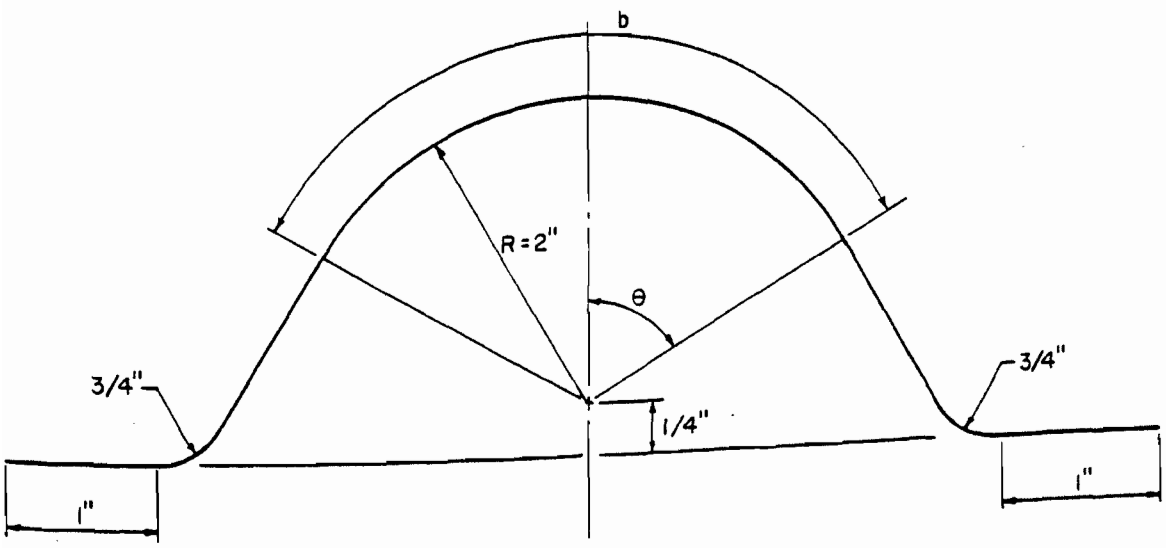

Fig. 3.5 D Profile

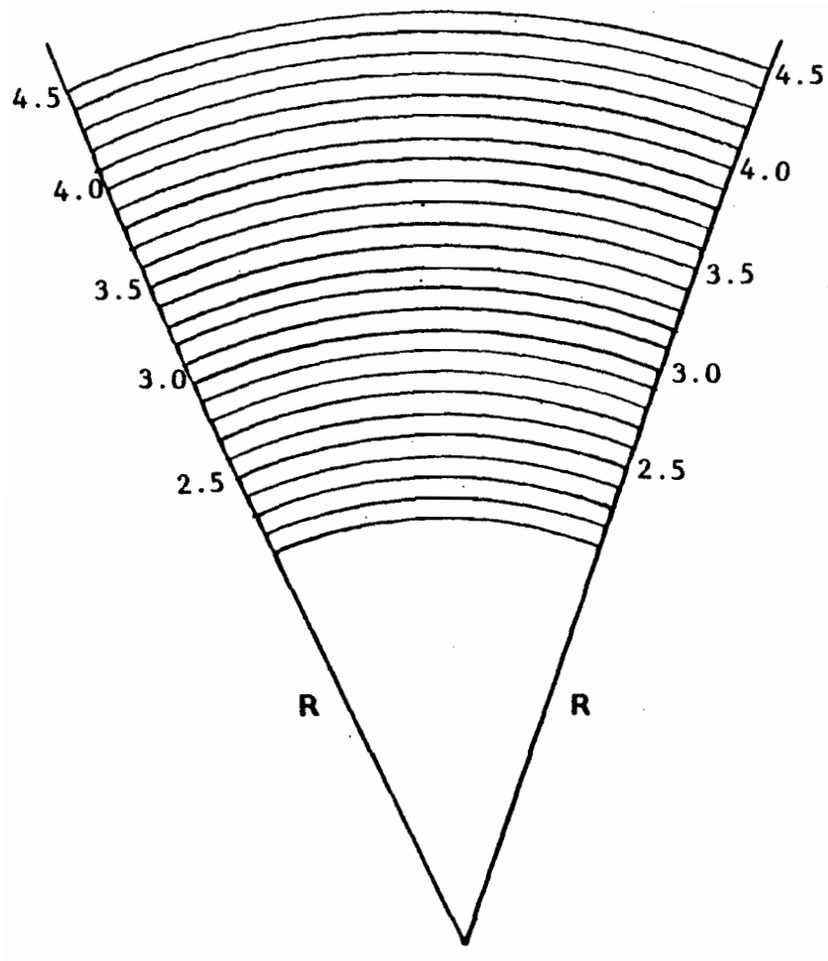

Fig. 3.6 Radius Gage for CS1 Specimens

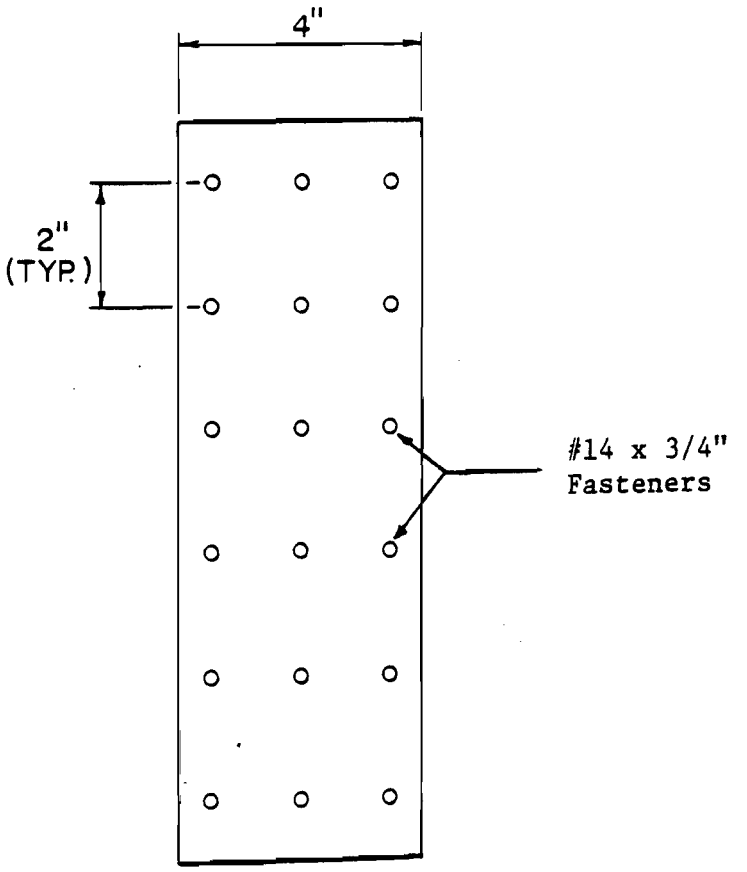

Fig. 3.7 Fastener Arrangement in the Web of CS (Stub Column) Specimens

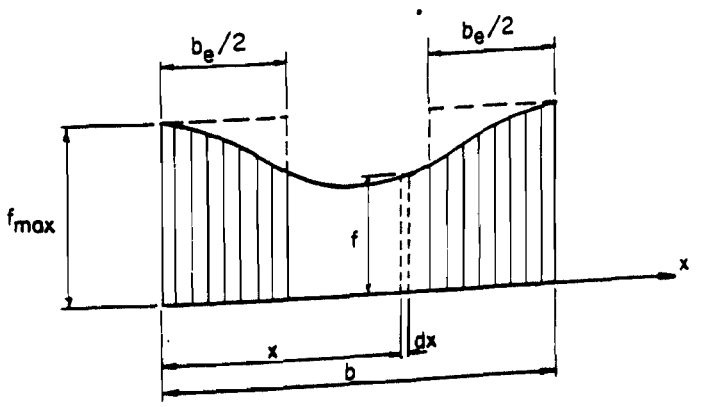

Fig. 3.8 Assumed Stress Variation in the Web After Buckling

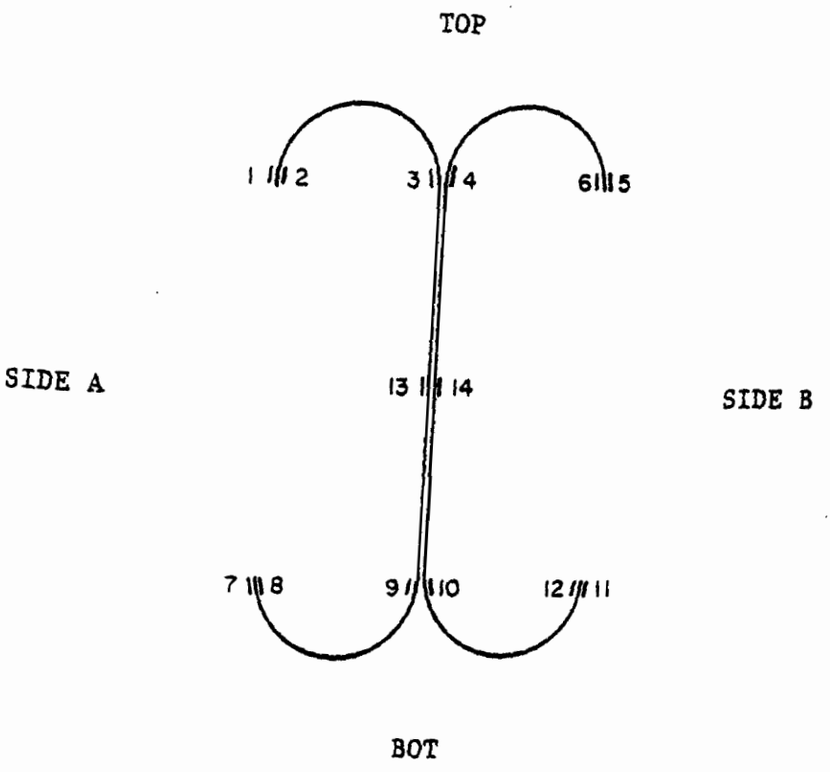

Fig. 3.9 Location of Strain Gages on Stub Column Specimens

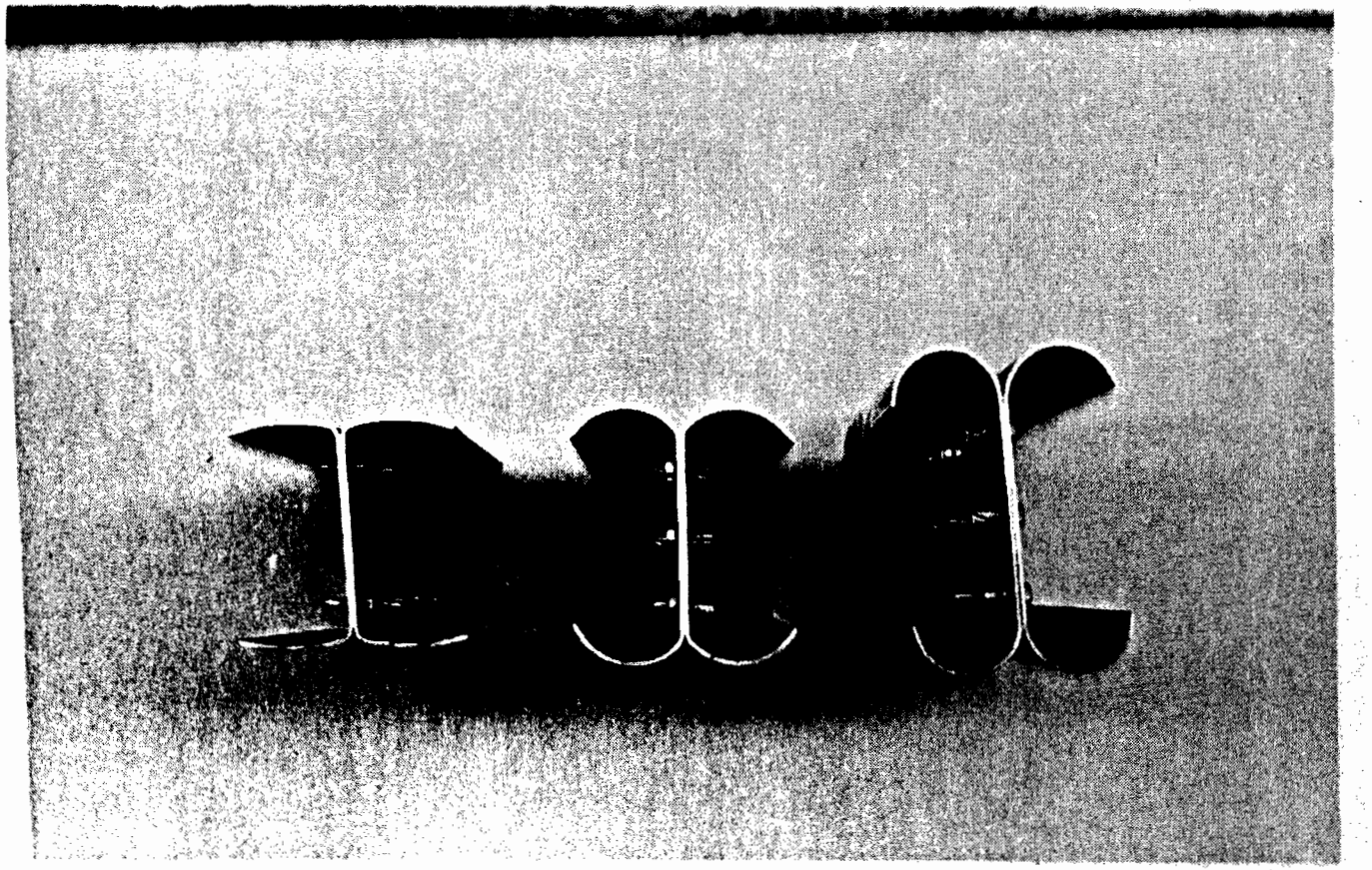

Fig. 3.10 Three Different Radii for the CS Specimen

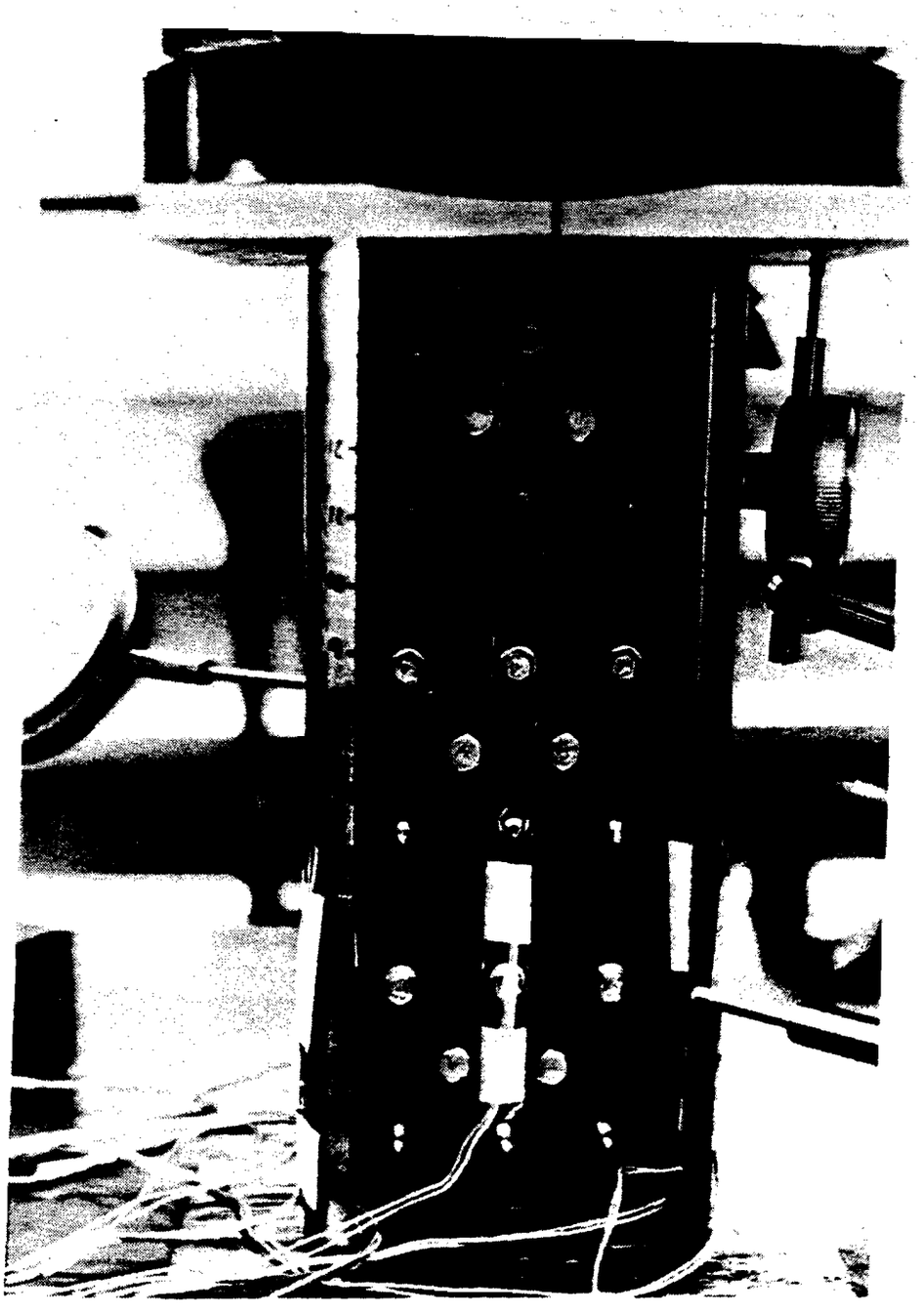

Fig. 3.11 Attachment of Web Bracing to Stub Column Specimens

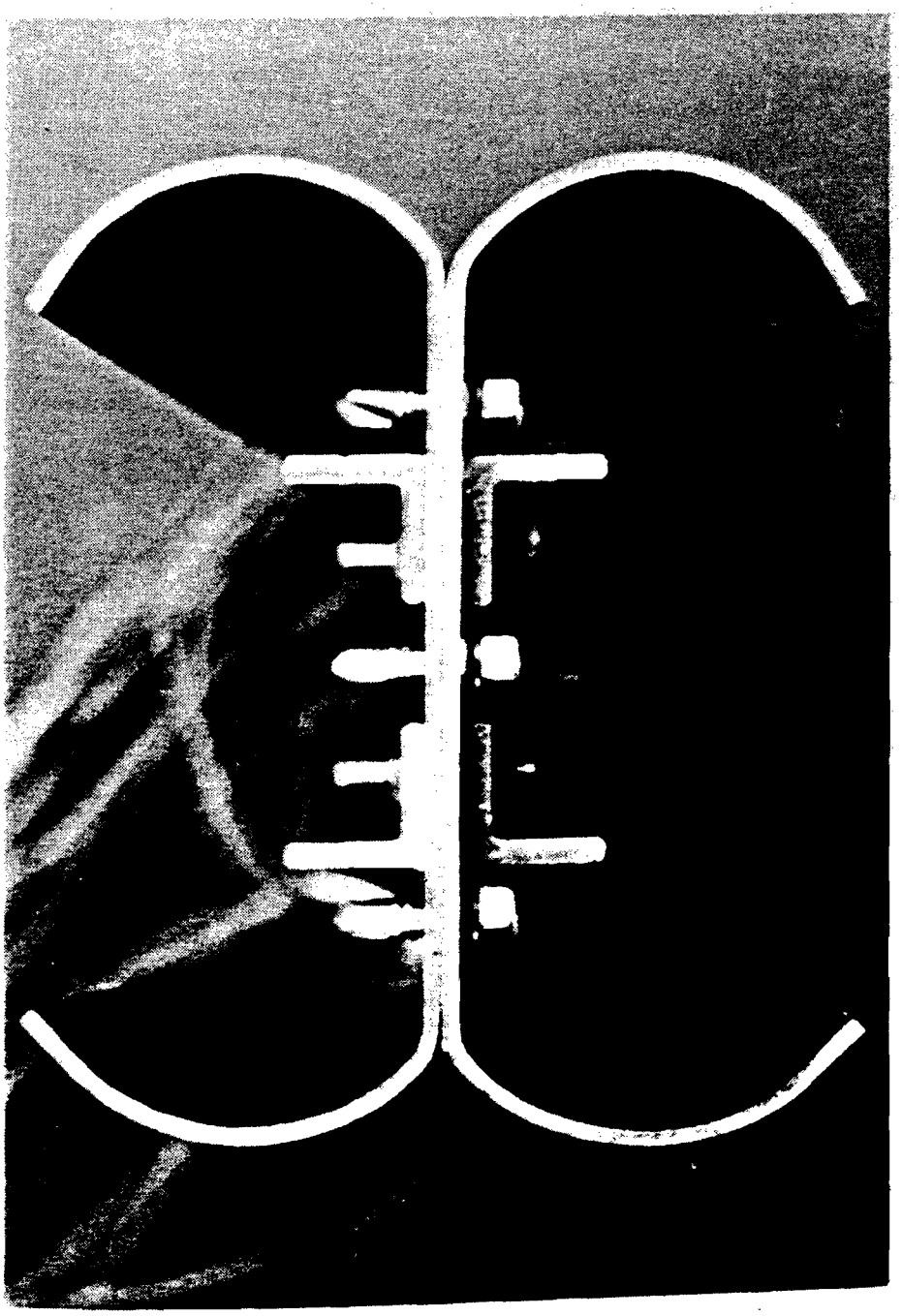

Fig. 3.12 Top View of Web Bracing

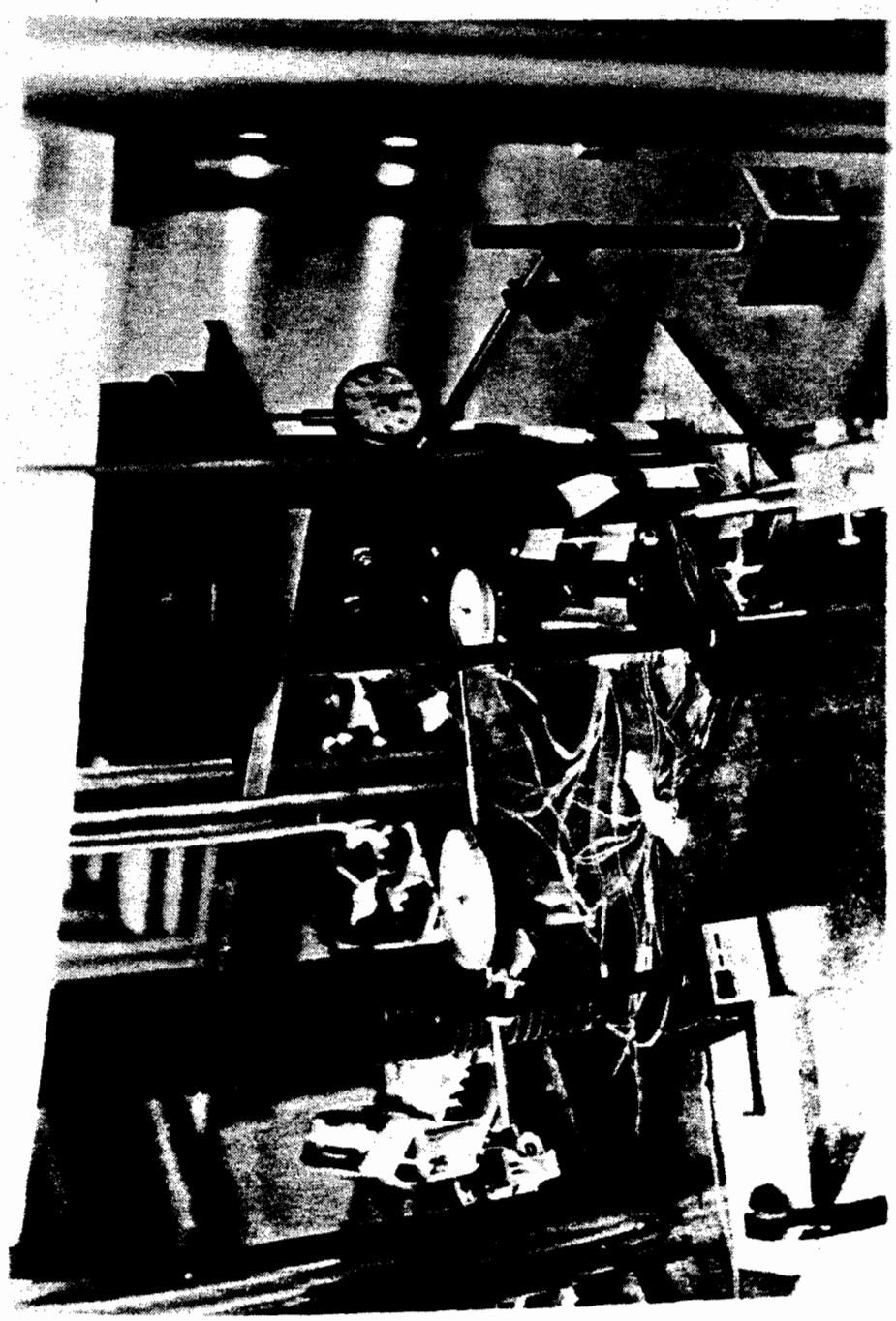

Fig. 3.13 Stub Column Test Setup Before Loading

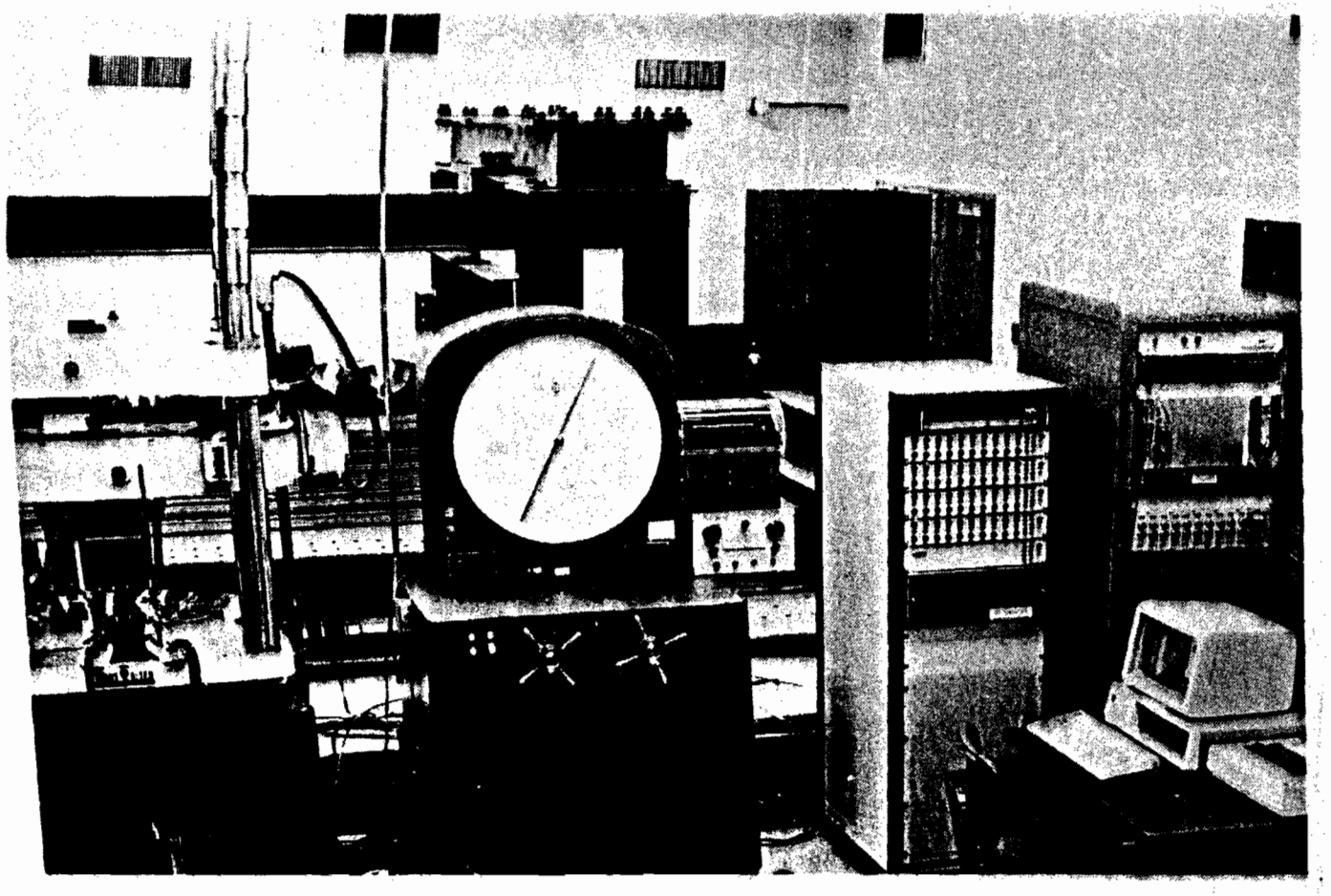

Fig. 3.14 Equipment Used in Stub Column Tests

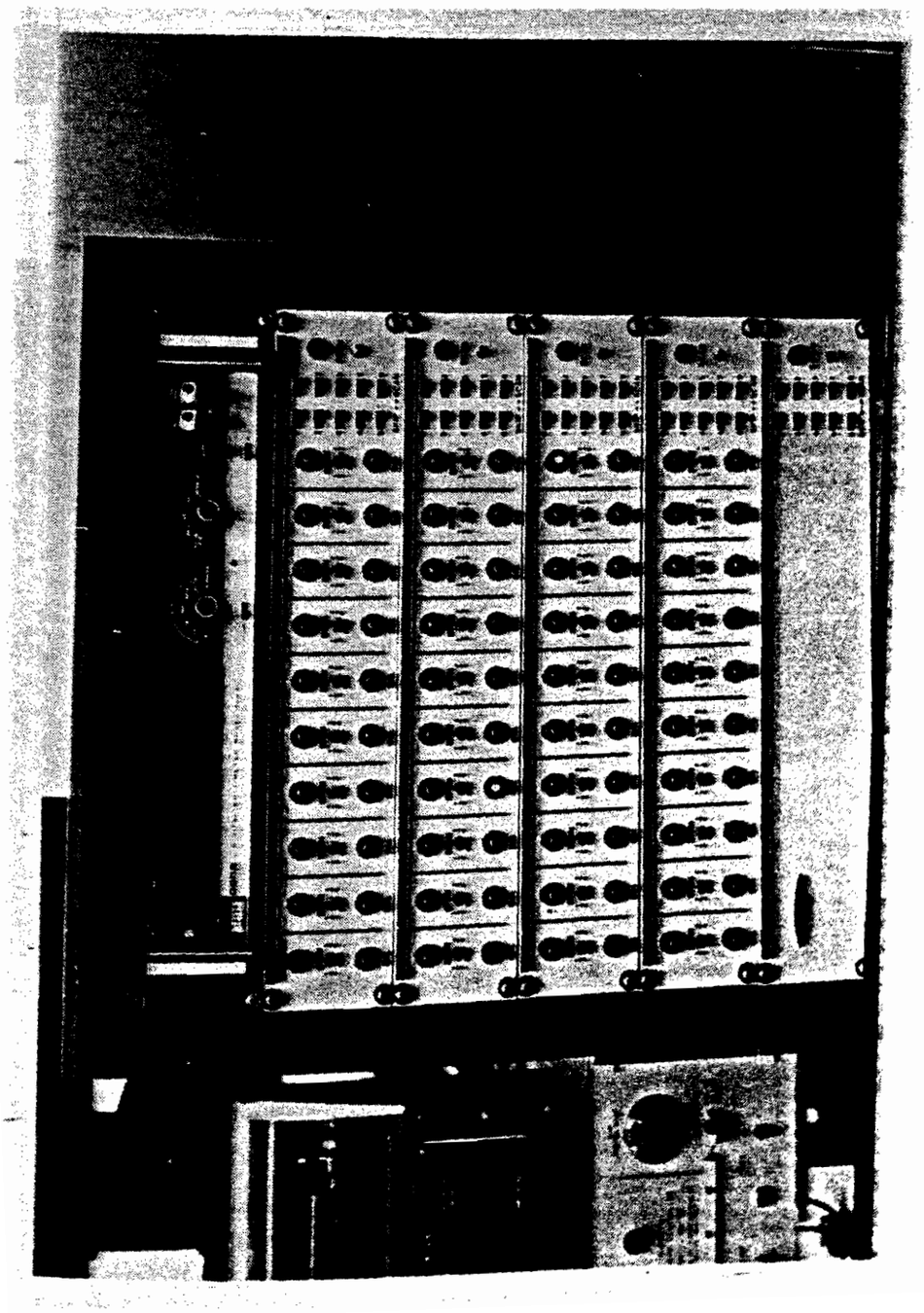

Fig. 3.15 40 Channel, Electronics/Ltd. Data Acquisition System

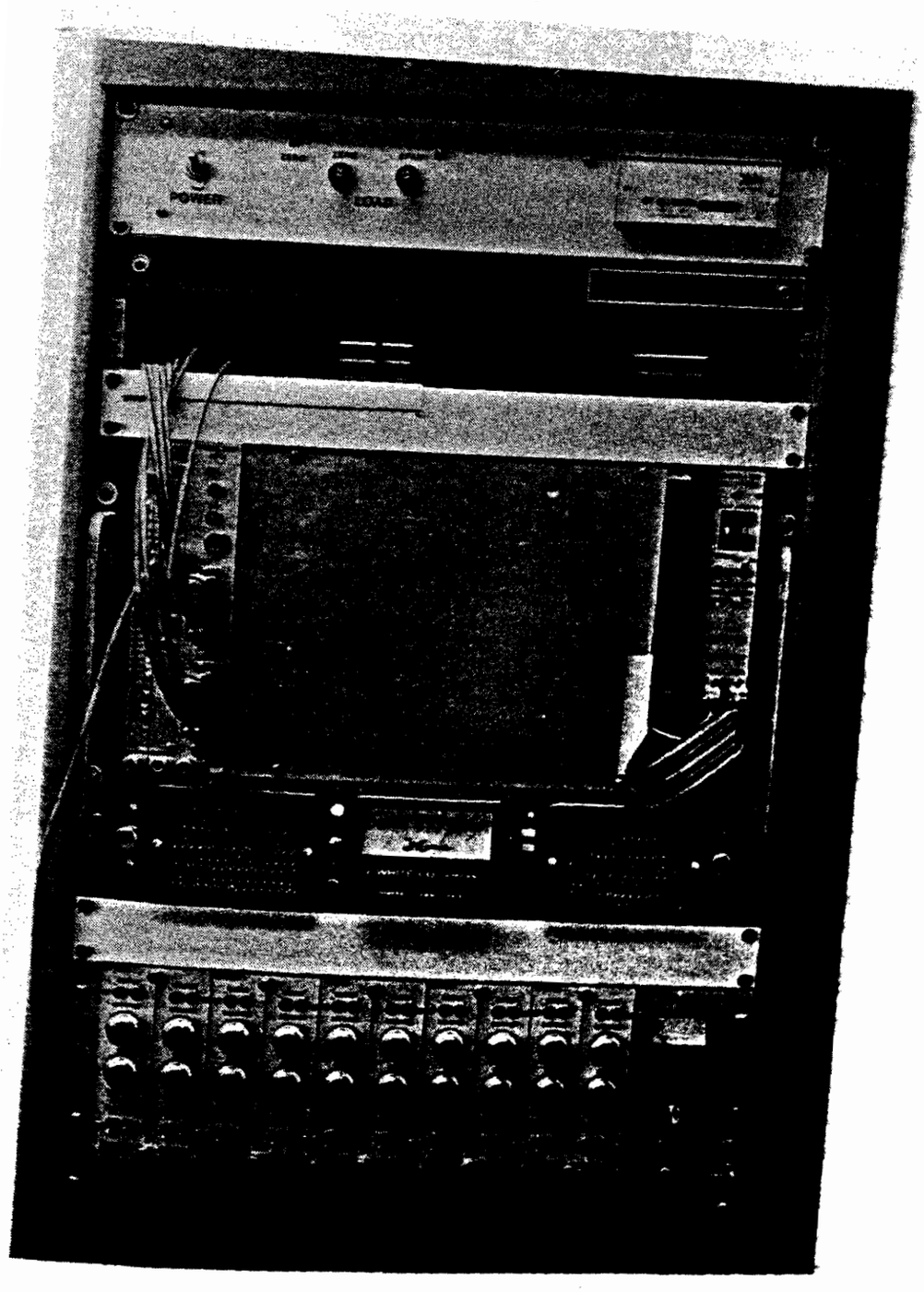

Fig. 3.16 Data Acquisition System Used for Load and Waving

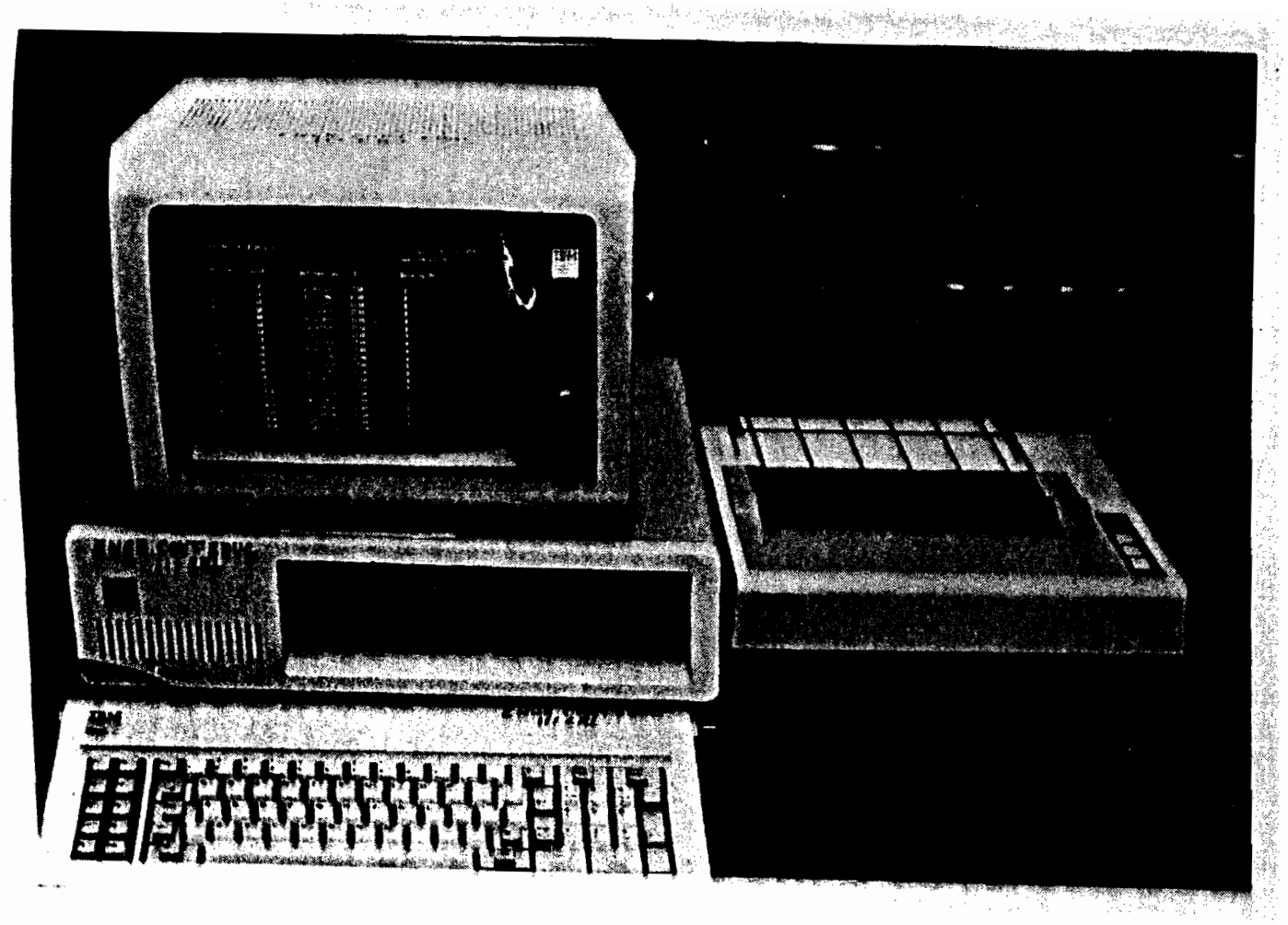

Fig. 3.17 IBM Personal Computer

Fig. 3.18 Typical Failure of the CS3 and CS2 Specimens

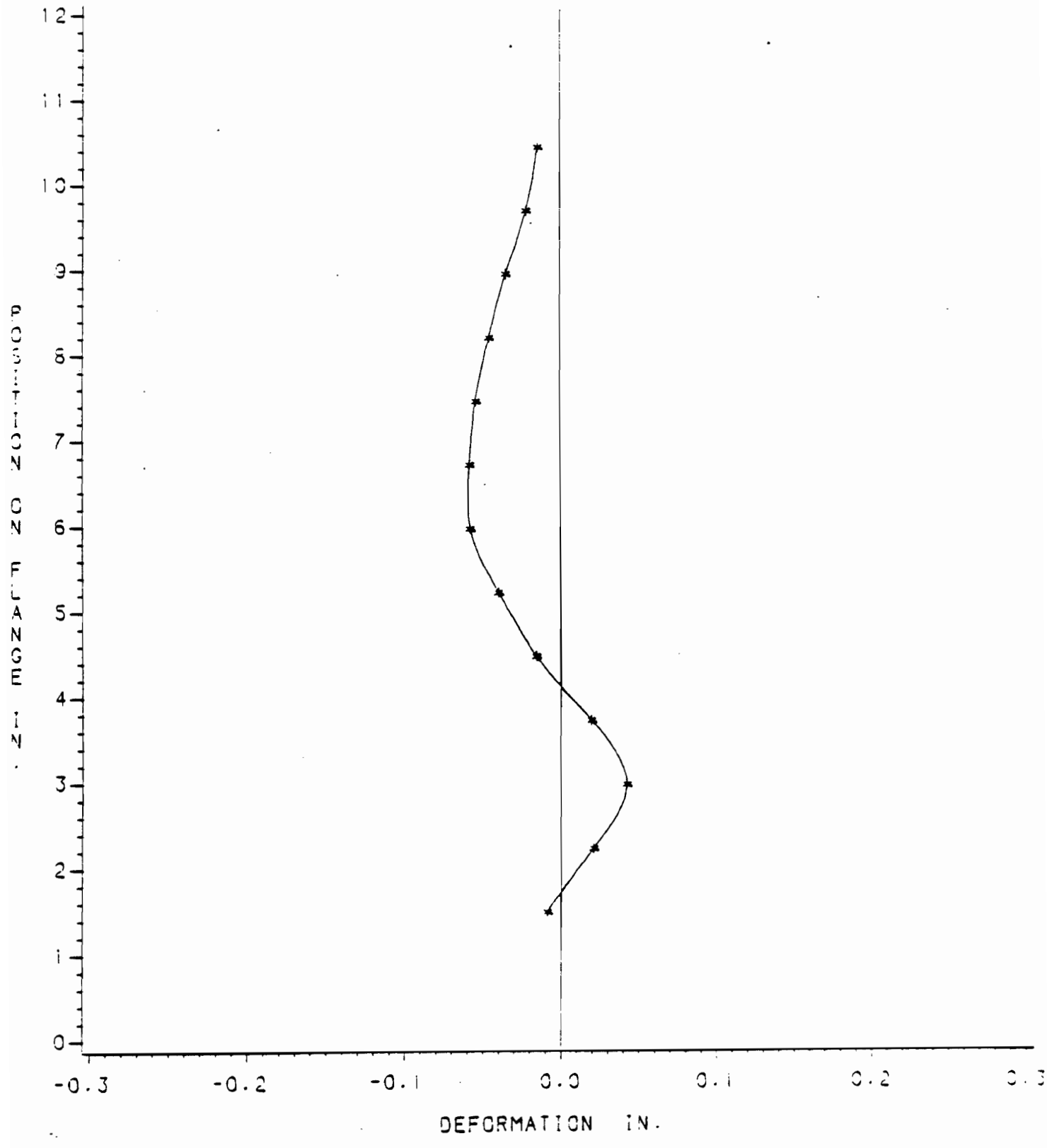

Fig. 3.19 Typical Wave Pattern for the CS3 Specimens Just Before Initial Buckling

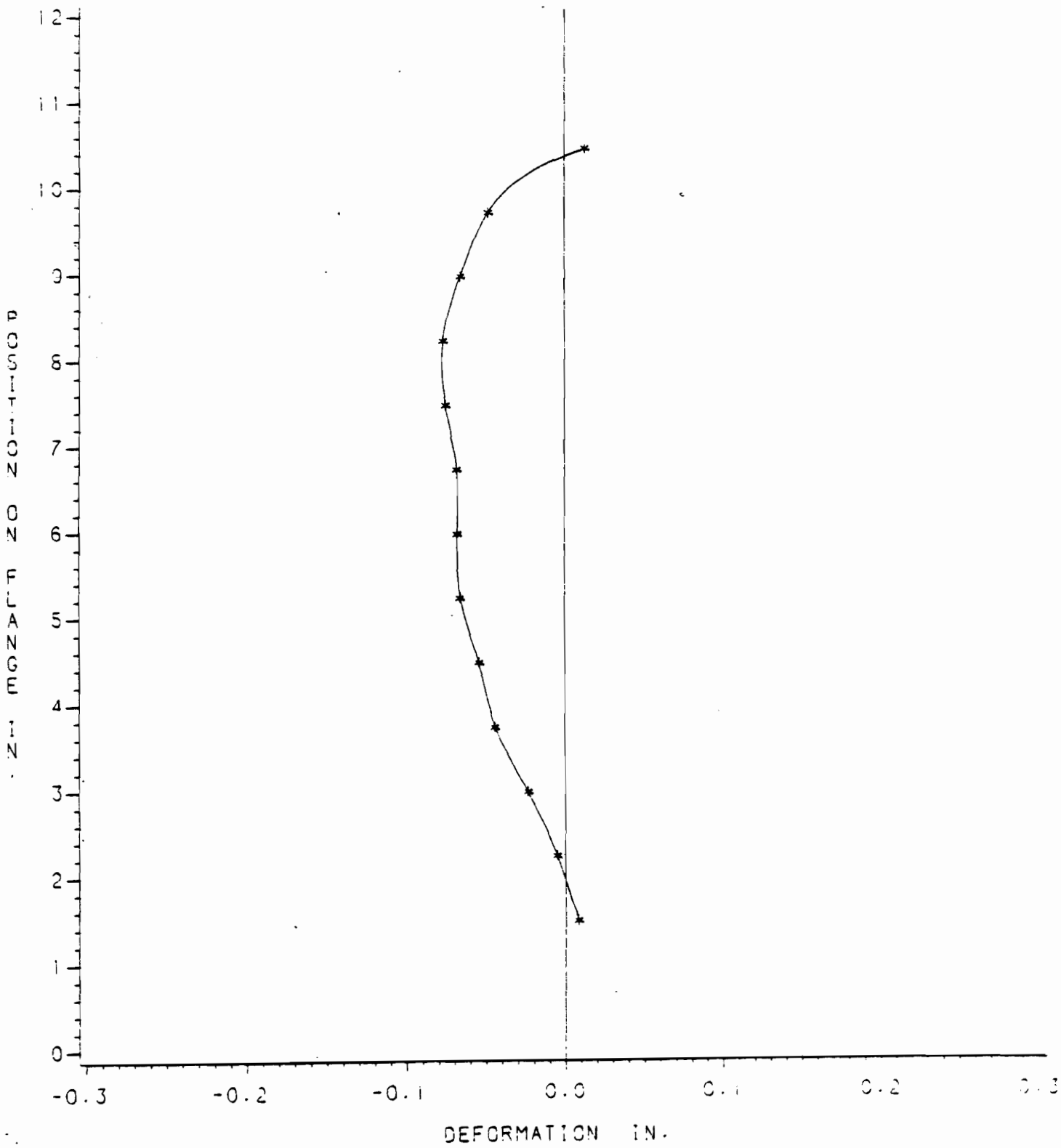

Fig. 3.20 Typical Wave Pattern for the CS2 Specimens Just Before Initial Buckling

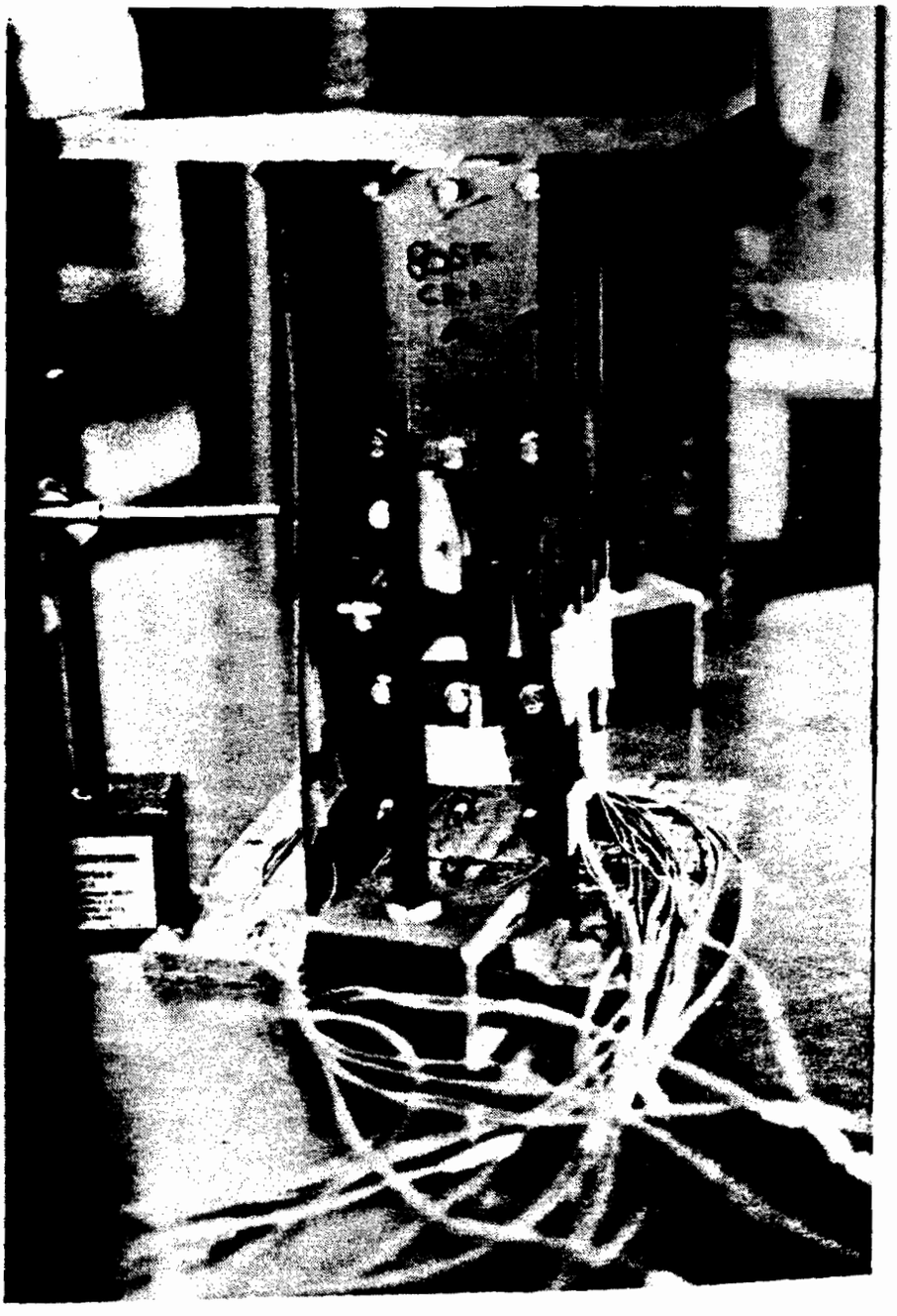

Fig. 3.21 Typical Failure of the CS1 Specimens

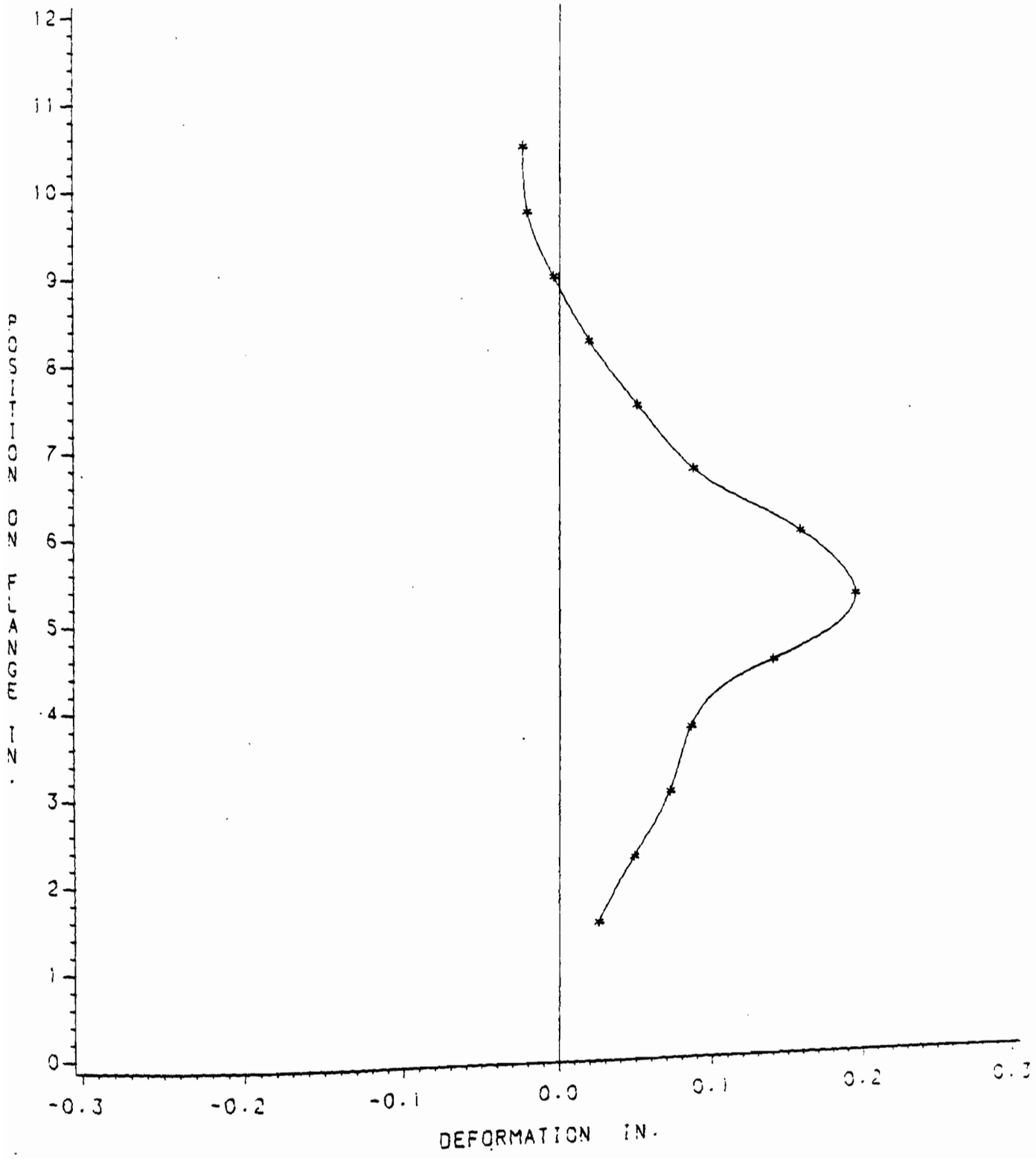

Fig. 3.22 Typical Wave Pattern for the CS1 Specimens Just Before Ultimate Load

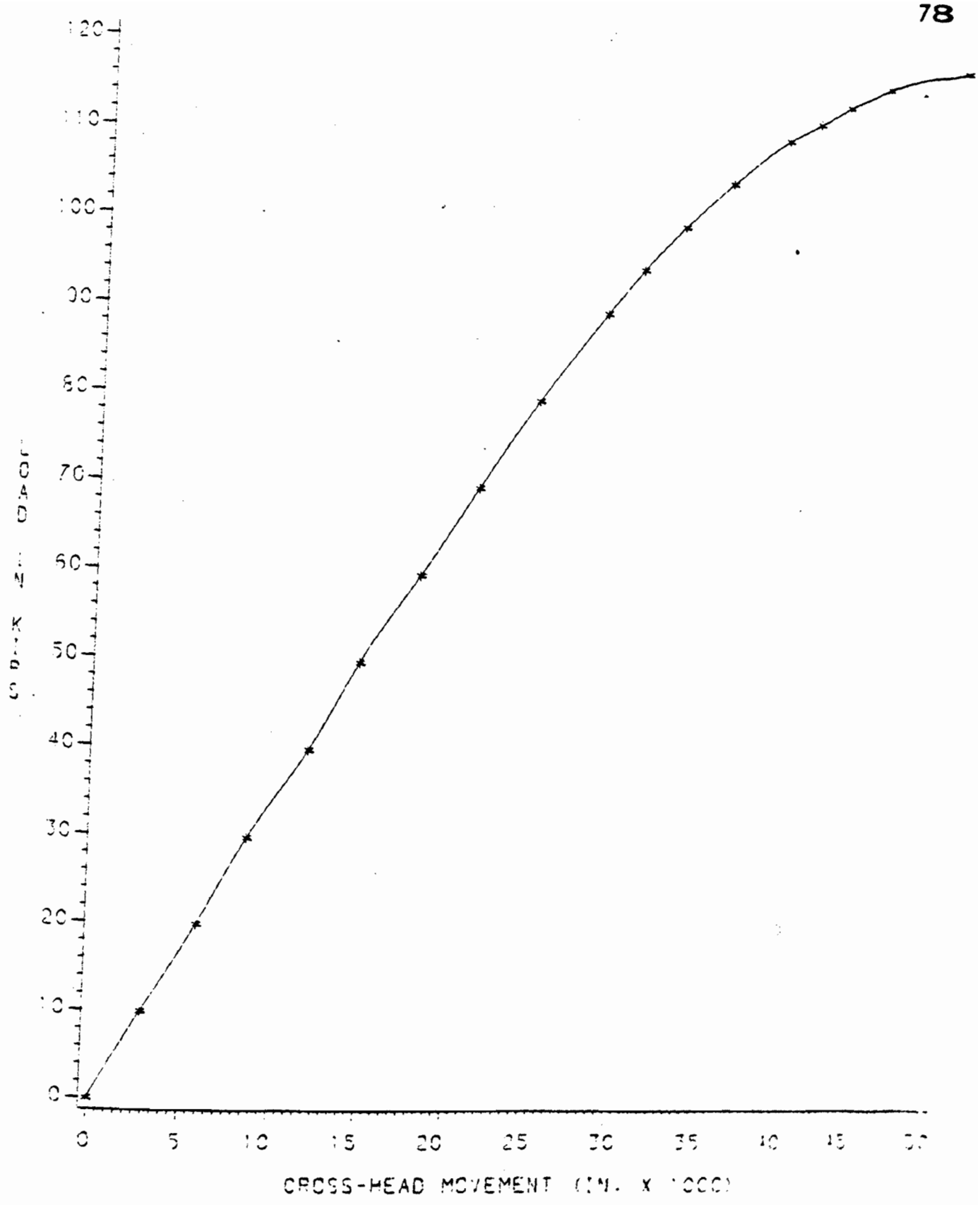

Fig. 3.23 Plot of Load Versus Cross-Head Movement for 80XFCS2-1 Specimen

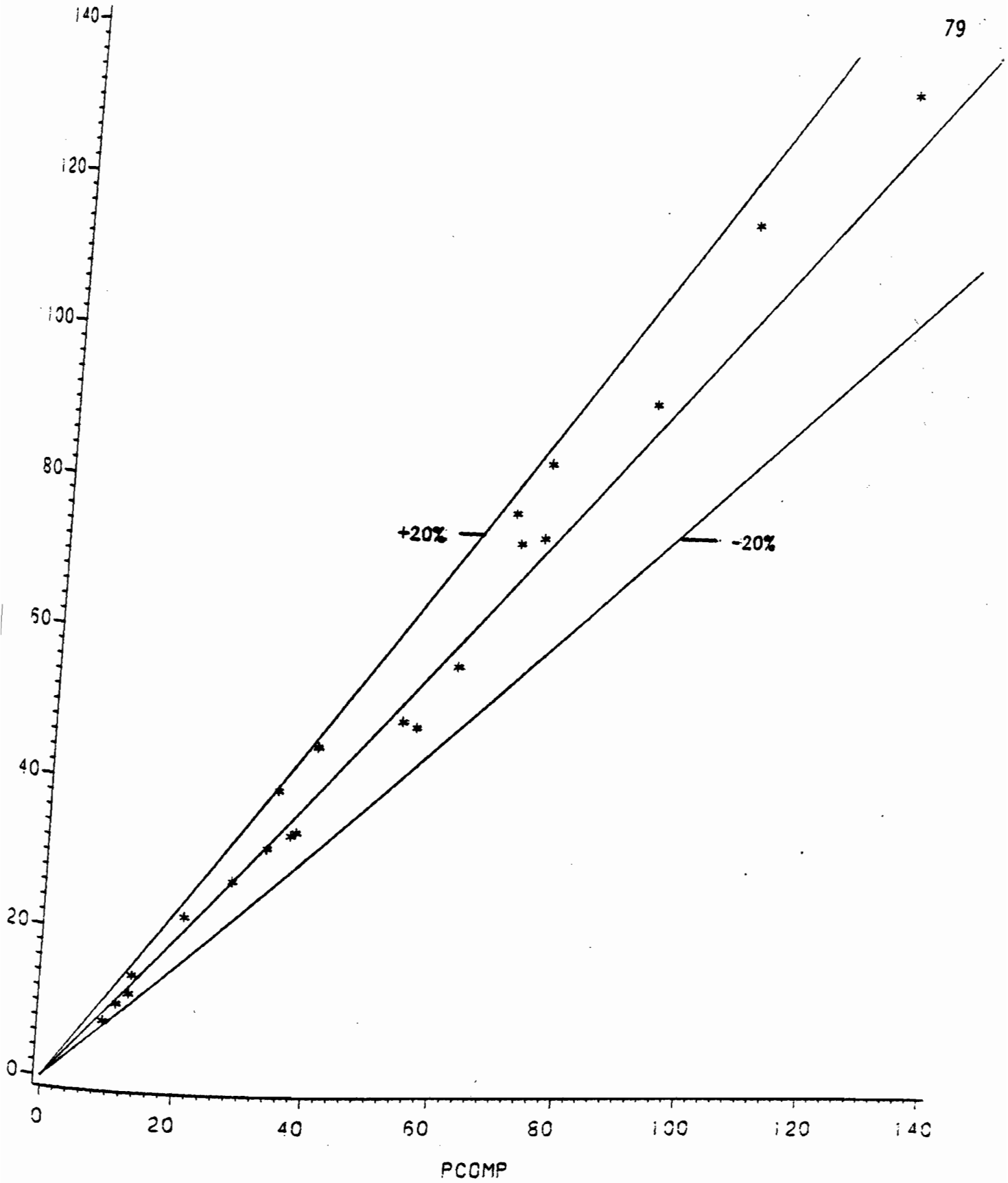

PINI = INITIAL BUCKLING LOAD OF CURVED ELEMENT

PCOMP = PREDICTED BUCKLING LOAD

Fig. 3.24 Plot of Initial Buckling Vs. Predicted Loads for Initial Curved Element Buckling

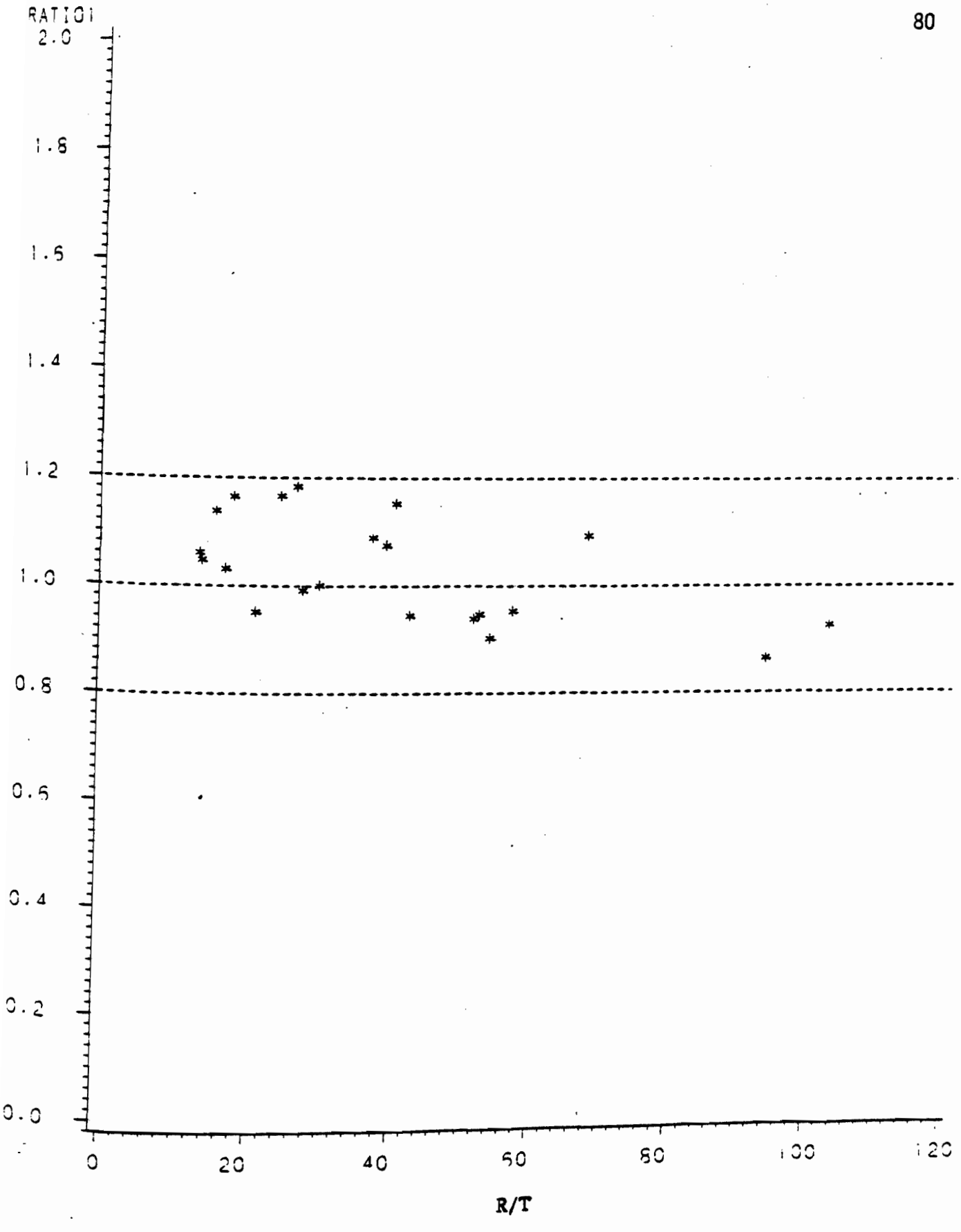

RATIO1=PINi/PCOMP
PINi = INITIAL BUCKLING LOAD
PCOMP = PREDICTED BUCKLING LOAD

Fig. 3.25 Plot of P_{ini}/P_{comp} Vs. R/t for Initial Curved Element Buckling

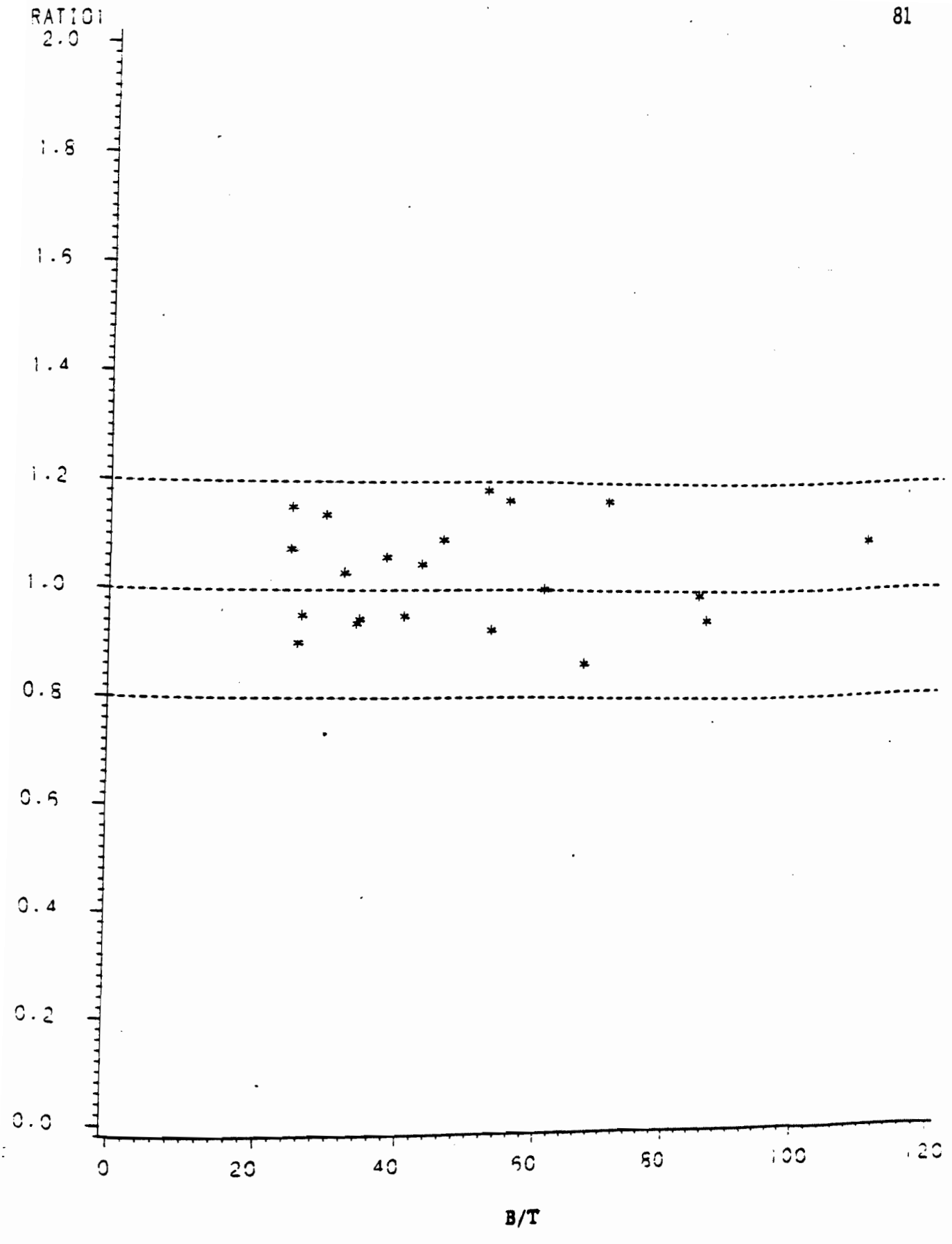

RATIO1=PINI/PCOMP
PINI = INITIAL BUCKLING LOAD
PCOMP = PREDICTED BUCKLING LOAD

Fig. 3.26 Plot of P_{ini}/P_{comp} Vs. b/t for Initial Curved Element Buckling

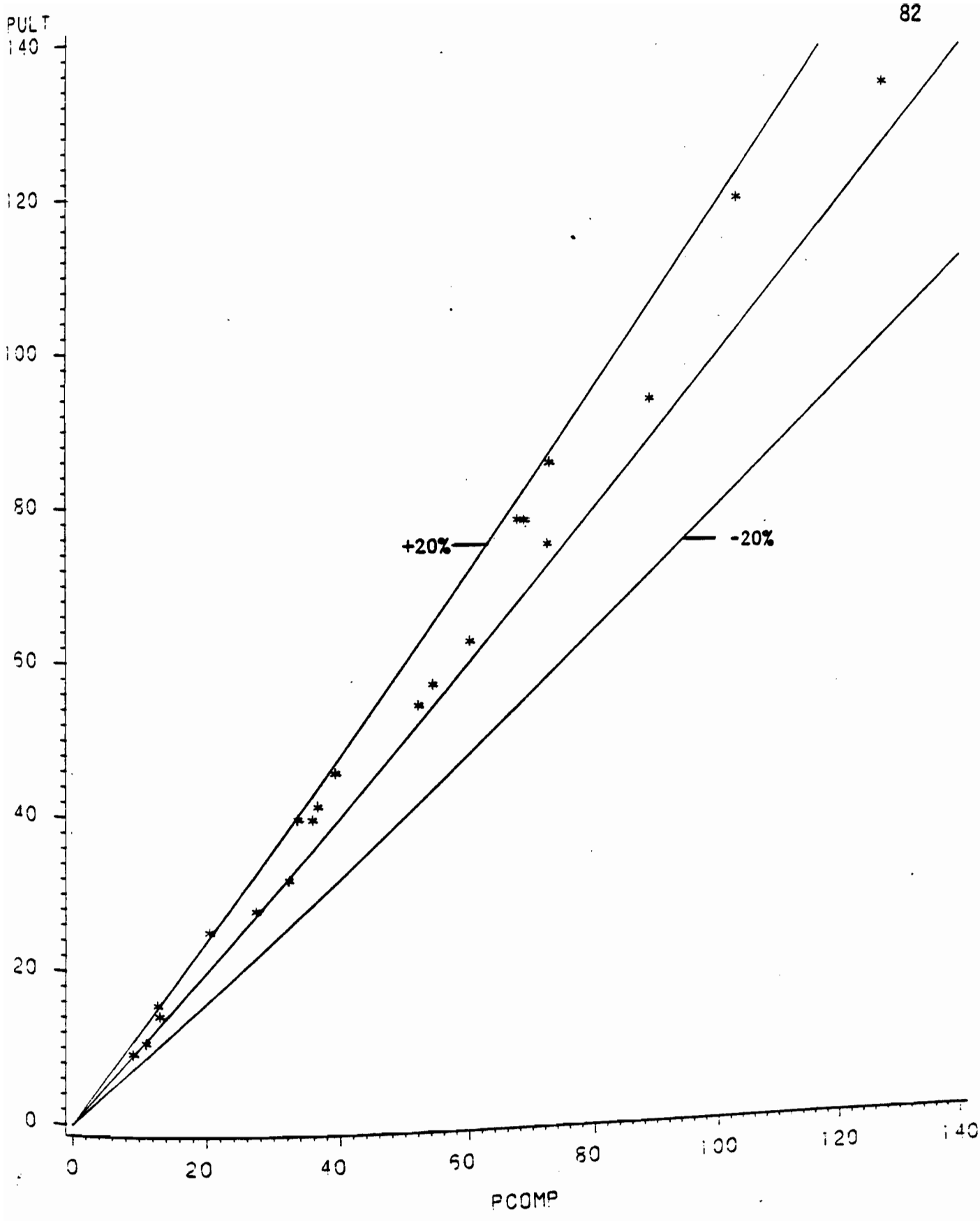

PULT = ULTIMATE LOAD THAT SPECIMEN COULD WITHSTAND

PCOMP = PREDICTED BUCKLING LOAD

Fig. 3.27 Plot of Ultimate Vs. Predicted Loads for Initial Curved Element Buckling

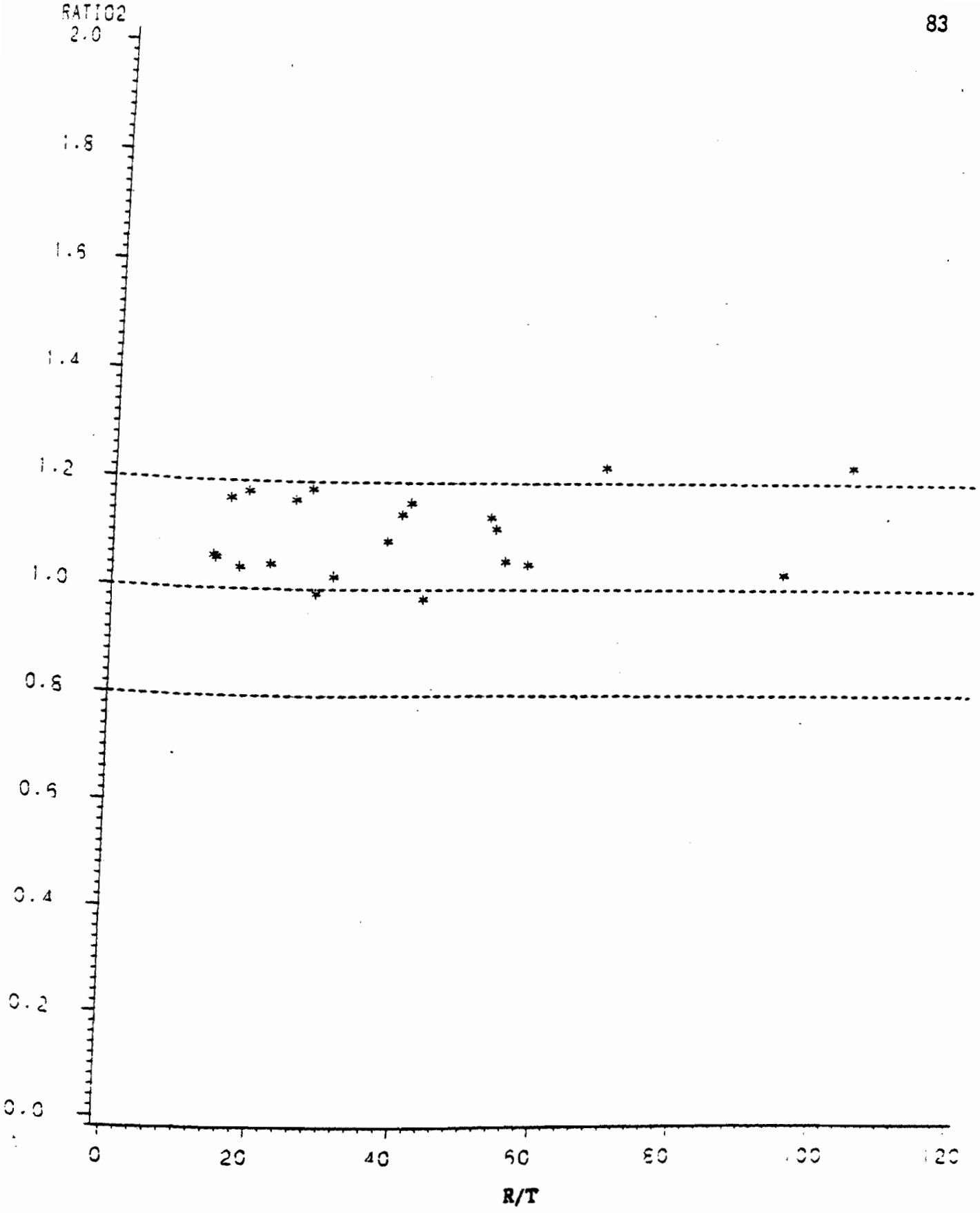

RATIO2=PULT/PCOMP
PULT = ULTIMATE LOAD
PCOMP = PREDICTED BUCKLING LOAD

Fig. 3.28 Plot of P_{ult}/P_{comp} Vs. R/t for Initial Curved Element Buckling

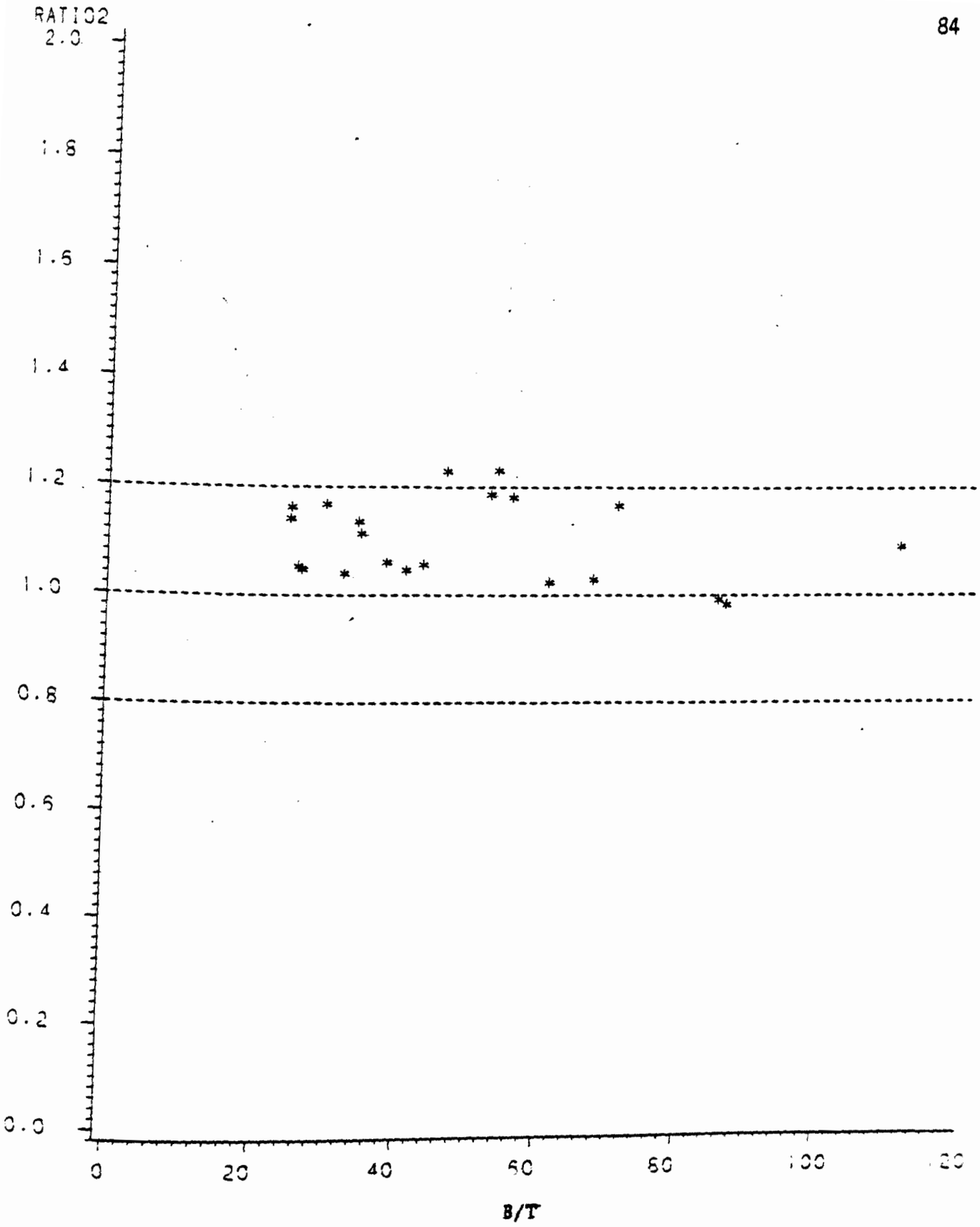

RATIO2=PULT/PCOMP
PULT = ULTIMATE LOAD
PCOMP = PREDICTED BUCKLING LOAD

Fig. 3.29 Plot of P_{ult}/P_{comp} Vs. b/t for Initial Curved Element Buckling

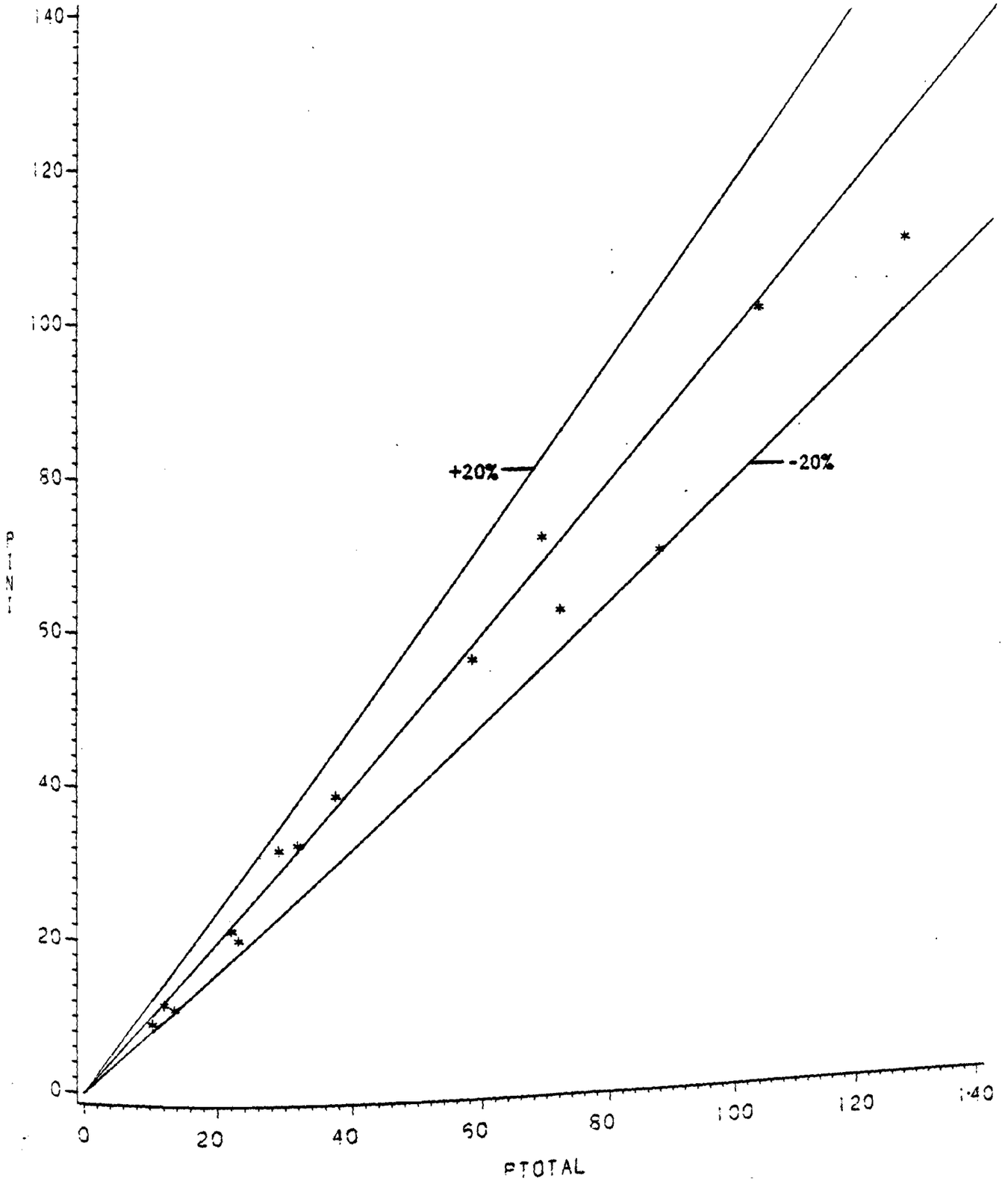

PINI = INITIAL BUCKLING LOAD OF CURVED ELEMENT

PTOTAL = PREDICTED TOTAL LOAD

Fig. 3.30 Plot of Initial Buckling Vs. Predicted Loads for Initial Flat Element Buckling

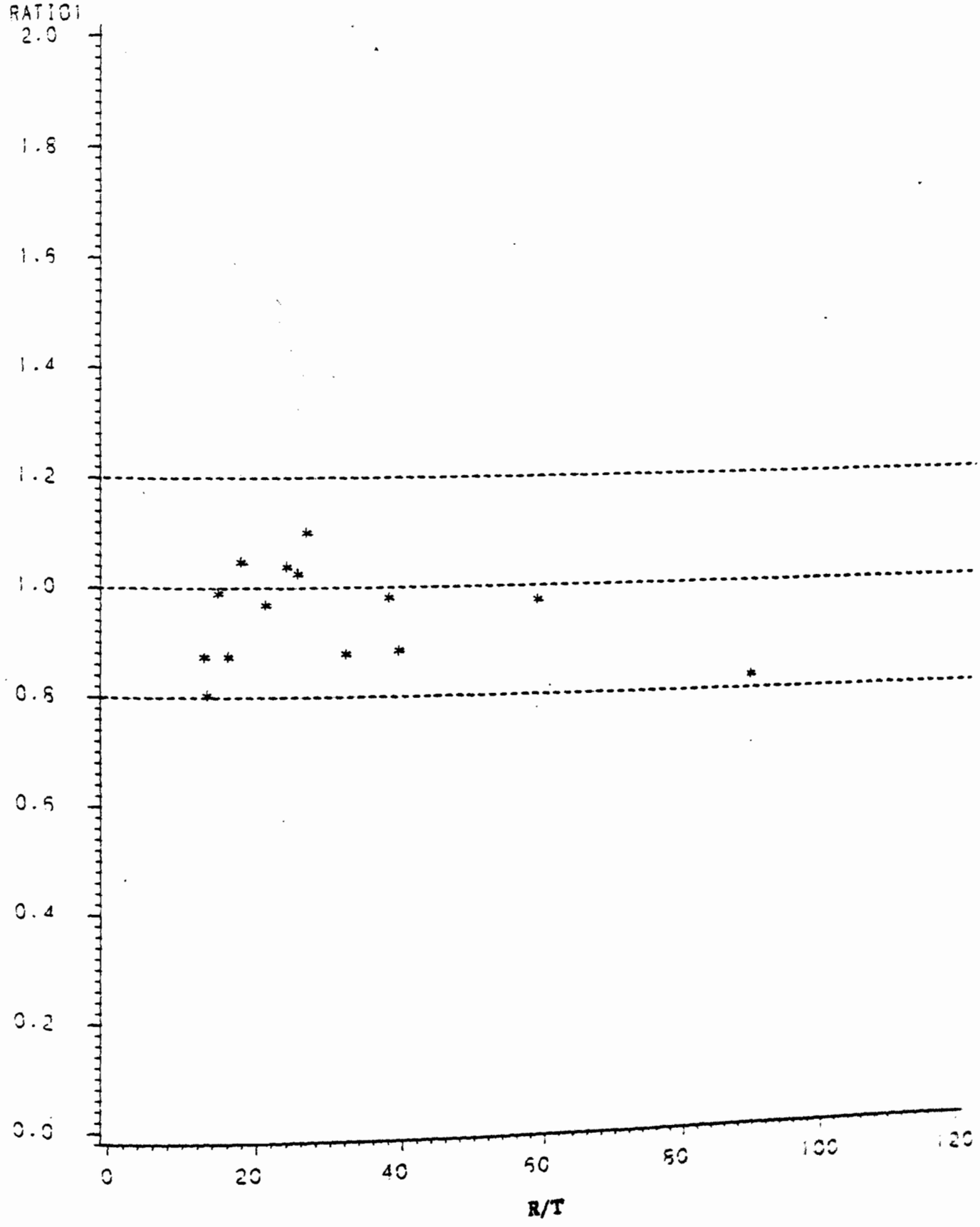

RATIO1=PINi/PTOTAL
PINi = INITIAL BUCKLING LOAD OF CURVED ELEMENT
PTOTAL = PREDICTED TOTAL FAILURE LOAD

Fig. 3.31 Plot of P_{ini}/P_{total} Vs. R/t for Initial Flat Element Buckling

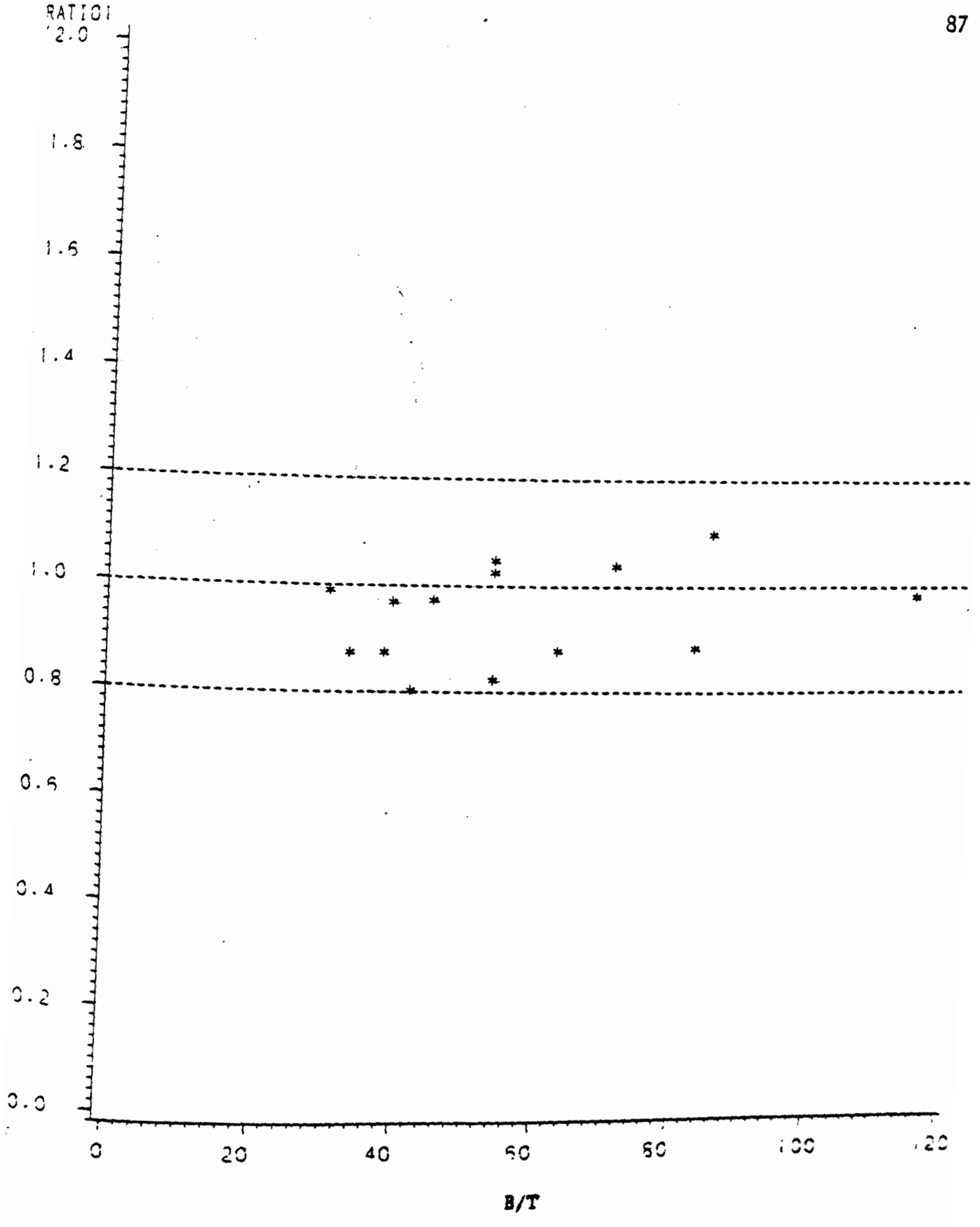

RATIO1=PINi/PTOTAL
PINi = INITIAL BUCKLING LOAD OF CURVED ELEMENT
PTOTAL = PREDICTED TOTAL FAILURE LOAD

Fig. 3.32 Plot of P_{ini}/P_{total} Vs. b/t for Initial Flat Element Buckling

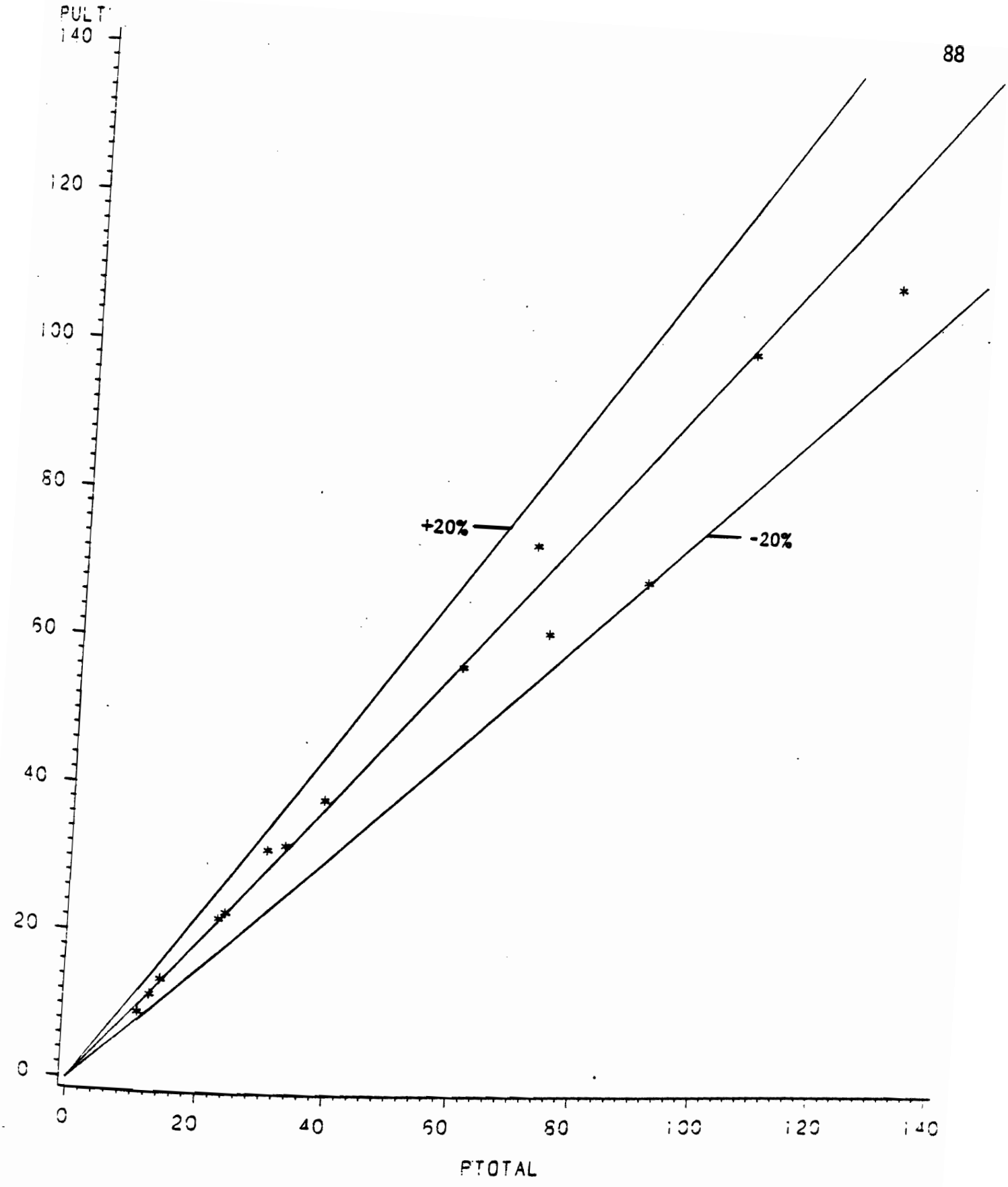

PULT = ULTIMATE LOAD THAT SPECIMEN COULD WITHSTAND

PTOTAL = PREDICTED TOTAL LOAD

Fig. 3.33 Plot of Ultimate Vs. Predicted Loads for Initial Flat Element Buckling

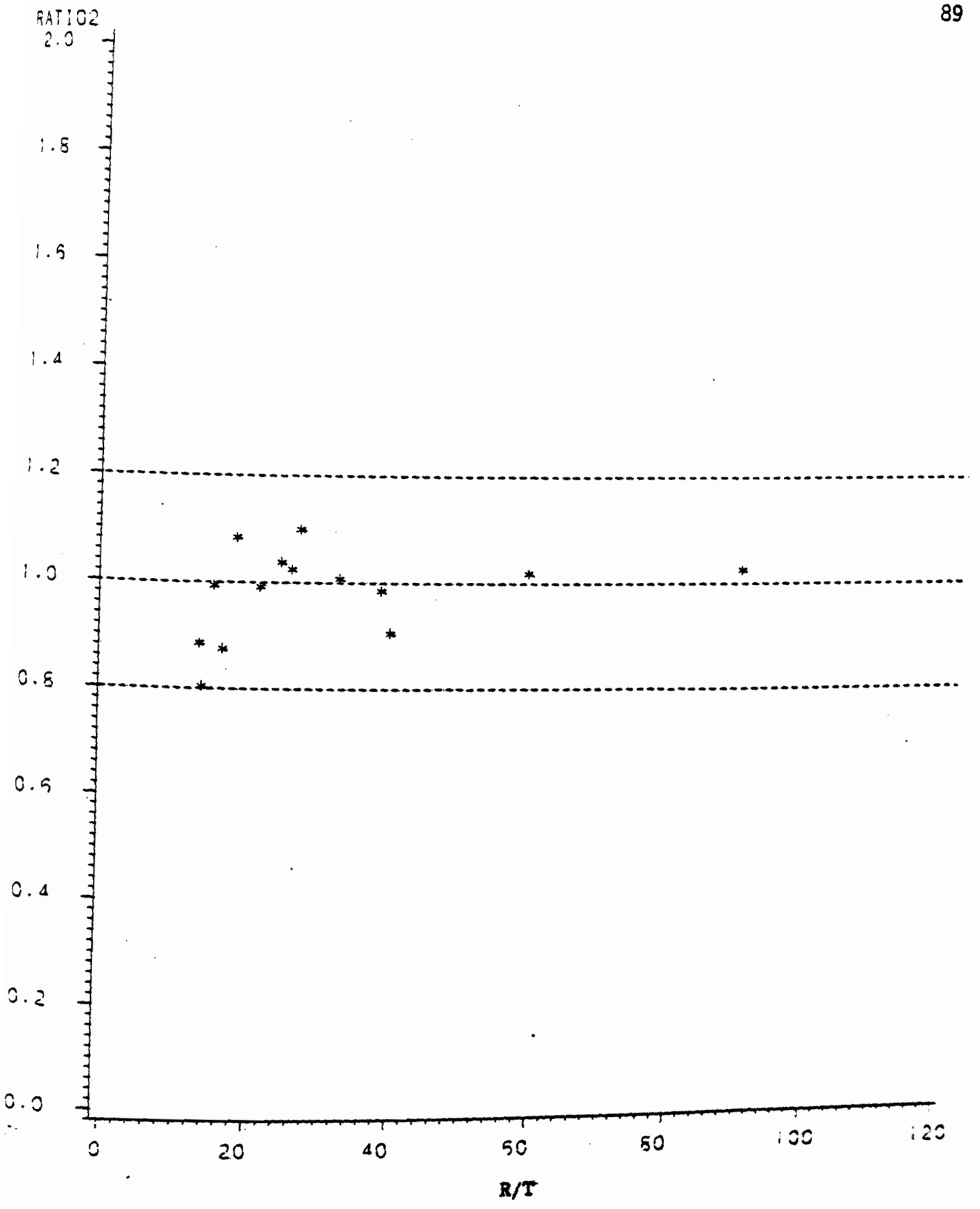

RATIO2=PULT/PTOTAL
PULT = ULTIMATE LOAD RESISTED BY SECTION
PTOTAL = PREDICTED TOTAL FAILURE LOAD

Fig. 3.34 Plot of P_{ult}/P_{total} Vs. R/t for Initial Flat Element Buckling

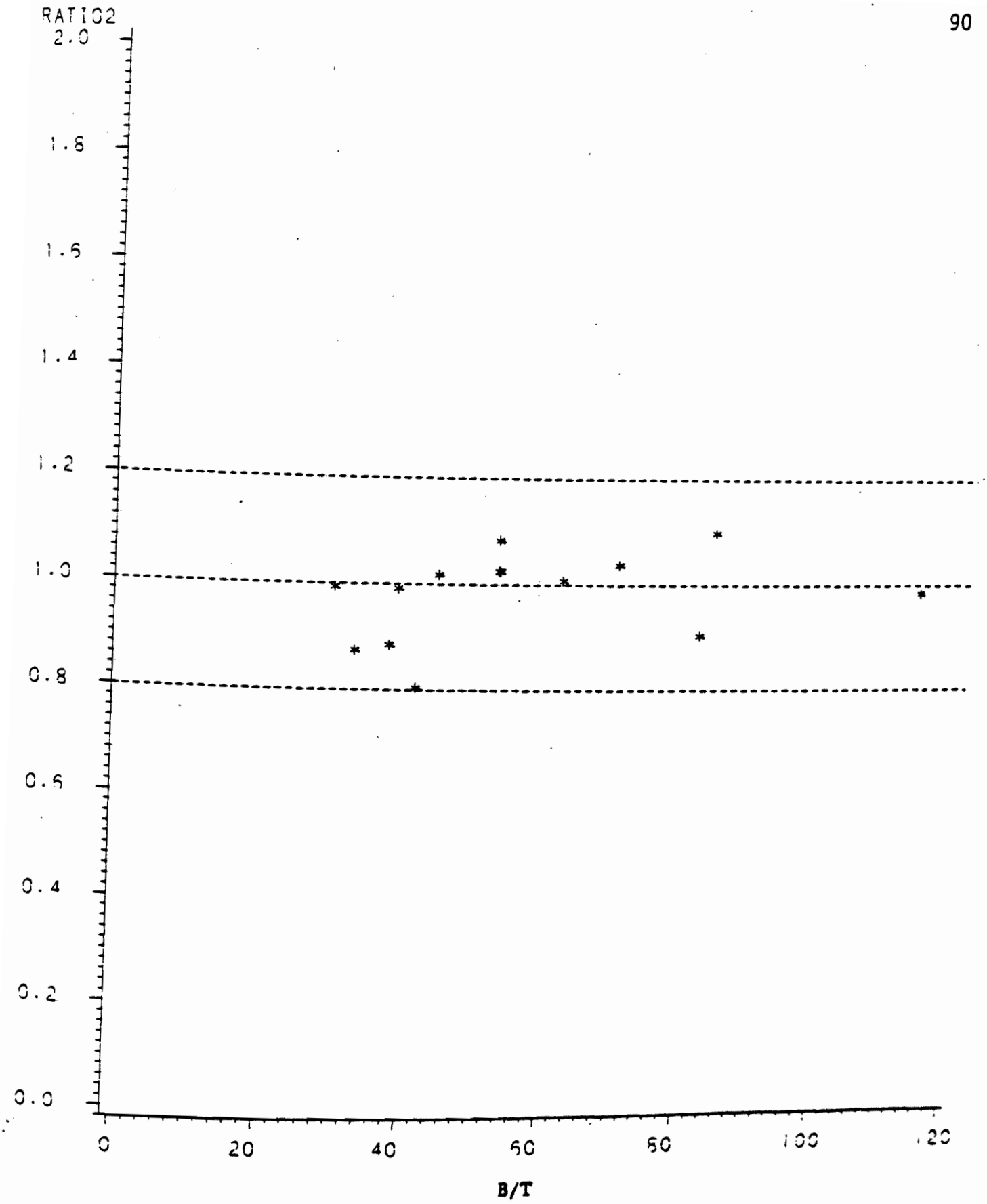

RATIO2=PULT/PTOTAL
PULT = ULTIMATE LOAD RESISTED BY SECTION
PTOTAL = PREDICTED TOTAL FAILURE LOAD

Fig. 3.35 Plot of P_{ult}/P_{total} Vs. b/t for Initial Flat Element Buckling

APPENDIX - NOTATION

The following symbols are used in this report:

A_i = area of i^{th} element;

b = curved element arc length;

b_e = flat element effective width;

E = modulus of elasticity;

f = actual stress at the edge of a flat compression element;

f_{cri} = elastic buckling stress of i^{th} element;

f_{cr} = predicted buckling stress of a curved element;

$(f_{cr}/E)_c$ = buckling stress ratio of a full cylinder with the same R/t ratio as the curved element;

$(f_{cr}/E)_f$ = buckling stress ratio of a simply supported flat plate with the same t/b ratio as the curved element;

$(f_{cr}/E)_p$ = buckling stress ratio of a simply supported curved element subject to uniform compression;

$(f_{cr}/E)_{pm}$ = buckling stress ratio of an unstiffened curved element subject to uniform compression;

F_{pr} = proportional limit;

F_y = yield strength;

F_u = ultimate strength;

R = curved element radius;

t = curved element thickness;

w = full width of a compression element;

μ = elastic Poisson's ratio;

θ = angle between the centerline and tangent of the D specimens as shown in Fig. 3.5;